

promoting access to White Rose research papers



Universities of Leeds, Sheffield and York
<http://eprints.whiterose.ac.uk/>

This is a copy of the final published version of a paper published via gold open access in **Earth and Planetary Science Letters**.

This open access article is distributed under the terms of the Creative Commons Attribution Licence (<http://creativecommons.org/licenses/by/3.0>), which permits unrestricted use, distribution, and reproduction in any medium, provided the original work is properly cited.

White Rose Research Online URL for this paper:
<http://eprints.whiterose.ac.uk/78529>

Published paper

Livingstone, SJ, Clark, CD and Tarasov, L (2013) Modelling North American palaeo-subglacial lakes and their meltwater drainage pathways. *Earth and Planetary Science Letters*, 375. 13 - 33. Doi 10.1016/j.epsl.2013.04.017



Modelling North American palaeo-subglacial lakes and their meltwater drainage pathways[☆]



Stephen J. Livingstone^{a,*}, Chris D. Clark^a, Lev Tarasov^b

^a Department of Geography, Sheffield University, Sheffield, UK

^b Department of Physics and Physical Oceanography, Memorial University of Newfoundland and Labrador, Canada

ARTICLE INFO

Article history:

Received 12 December 2012

Received in revised form

8 April 2013

Accepted 12 April 2013

Editor: J. Lynch-Stieglitz

Available online 4 June 2013

Keywords:

subglacial lake

palaeo-subglacial lake

meltwater drainage pathways

Laurentide Ice Sheet

numerical ice-sheet modelling

geomorphology

ABSTRACT

This paper presents predictions of palaeo-subglacial lakes and their drainage pathways beneath the North American Ice Sheet during the last glaciation. We utilise data on the current topography and seafloor bathymetry, and elevation models of the ice- and ground-surface topography from data-calibrated glaciological modelling to calculate the hydraulic potential surface at the ice-sheets bed. Given that specific ice-surface elevations are only known from modelled outputs, and thus contain significant uncertainty, we utilise many such outputs to examine where on the bed that subglacial lakes are likely to have occurred. Our analysis demonstrates the potential for subglacial lake genesis, particularly beneath the former Cordilleran Ice Sheet; along the suture zone between the Laurentide and Cordilleran ice sheets; in Hudson Bay; in the Great Lake basins and deep trenches of the Canadian Archipelago. During the Last Glacial Maximum we suggest that at least 1000 km³ of meltwater could have been stored subglacially. As the ice-sheet and the bed evolved subglacial lakes repeatedly formed and emptied, particularly in Hudson Bay and the suture zone between the Laurentide and Cordilleran ice sheets where lakes were characteristically broad and shallow (< 10 m deep). In contrast, the Cordilleran Ice Sheet was characterised by deep (up to ~90 m) and persistent lake genesis. Significantly, similar distributions and modes of predicted subglacial lakes are obtained irrespective of the model or model run, which suggests the results are robust. Subglacial meltwater drainage varied between stable networks, typically associated with strong topographic controls, and convoluted networks that underwent considerable dynamism, including repeated meltwater network capture. These lake likelihood predictions could usefully form targets for detailed field and remote investigations and we hypothesise and explore the potential that numerous deposits and spillways previously interpreted as arising from ice-marginal lakes may have emanated from their subglacial cousins.

© 2013 The Authors. Published by Elsevier B.V. All rights reserved.

1. Introduction

The generation, storage and evacuation of meltwater plays a fundamental role in modulating the behaviour of ice masses (e.g. Hubbard et al., 1995; Joughin et al., 2008; Stearns et al., 2008; Bartholomew et al., 2010). Indeed, the link between subglacial meltwater and ice streaming is well documented (e.g. Engelhardt and Kamb, 1997; Smith et al., 2007). However, the spatial and temporal form of the meltwater network at the base of the Antarctic and Greenland ice sheets is not well known. This compromises our ability to accurately model processes at the ice-bed interface. An alternative approach is to observe marine and terrestrial palaeo-ice sheet beds to discern the composite imprint

of subglacial processes expressed in the geomorphological and sedimentological record. This includes meltwater channels eroded into bedrock or sediment, eskers and subglacial lake deposits. These glacial landforms can be investigated at a range of scales from detailed sedimentological analysis of individual bedforms to subcontinental-scale glacial geomorphological mapping (e.g. Prest et al., 1968; Banerjee and McDonald, 1975; Shilts et al., 1987; Gorrell and Shaw, 1991; Kleman, 1992; Clark and Walder, 1994; Punkari, 1997; Fisher et al., 2005; Kozłowski et al., 2005; Margold et al., 2011; Burke et al., 2012).

Subglacial lakes are commonplace beneath the Antarctic Ice Sheet (AIS), occurring at a range of scales in a variety of topographic, thermal and ice-dynamical settings, and comprising a significant and active component of the hydrological system (e.g. Smith et al., 2009; Wright and Siegert, 2011). It is likewise anticipated that subglacial lakes existed beneath the North American Ice Sheet (NAIS) during the Quaternary (see Livingstone et al., 2012) and therefore would have had a similar influence on ice dynamics and water flow. However, palaeo-subglacial lakes are

[☆]This is an open-access article distributed under the terms of the Creative Commons Attribution License, which permits unrestricted use, distribution, and reproduction in any medium, provided the original author and source are credited.

* Corresponding author. Tel.: +44 114222 7990.

E-mail address: s.j.livingstone@sheffield.ac.uk (S.J. Livingstone).

rarely documented (e.g. Gjessing, 1960; Munro-Stasiuk, 2003; Christoffersen et al., 2008; Lesemann and Brennand, 2009) and typically controversial (e.g. Evans et al., 2006) in part due to difficulties in distinguishing their geological signature from proglacial (ice-marginal or ice-fed) lakes (see Livingstone et al. (2012) for a review). In contrast, meltwater channels, tunnel valleys and eskers are widely observed across the formerly glaciated bed of North America, forming intricate networks detailing the composite history of meltwater drainage and ice-sheet behaviour (e.g. Bretz, 1923; Wright, 1973; Walder and Hallet, 1979; Shilts et al., 1987; Margold et al., 2011, 2013). Nevertheless, the temporal history of these features is poorly constrained throughout the evolution of the NAIS and therefore only provides a relative appreciation of meltwater flow. It is therefore difficult to elucidate when channels and eskers formed and over what time-scales they developed. Thus, despite the wealth of data, ease of access (both remotely and in the field) and spatial coverage, disentangling the glacial meltwater history of North America is complex.

With this in mind, we use hydraulic calculations derived using an ensemble of palaeo-ice and bed topographies from thermo-mechanical ice-sheet models to simulate subglacial meltwater routes and predict where meltwater may have ponded at the ice–bed interface. This builds upon the work of Evatt et al. (2006), who used a similar approach to predict subglacial lakes at the Last Glacial Maximum (LGM). The results are presented as a series of composite maps that allow us to evaluate (i) the broad-scale patterns of meltwater drainage and evolution; and (ii) the likelihood of subglacial lakes forming at a particular location. Meltwater drainage networks are simulated at discrete time-slices throughout the evolution of the last NAIS, which allows the spatial and temporal correlations between channels, subglacial lakes, and ice-streams to be investigated. And subglacial lake predictions provide a useful guide for detailed future field investigations and for elucidating their frequency, stability, and distribution through the ice-sheets evolution.

2. Generation of subglacial lake and meltwater drainage predictions

Three-dimensional (3D) hydraulic potential surfaces (Φ) were calculated for the bed of the NAIS during the last glaciation from current digital elevation models (DEMs) of the bed topography and seafloor bathymetry and simulated elevation models of the ice and ground surface topography, using the following equation (Shreve, 1972; Clarke, 2005):

$$\Phi = \rho_w g h_b + F \rho_i g H, \quad (1)$$

where ρ_w is the density of water (1000 kg m^{-3}); ρ_i is the density of ice (917 kg m^{-3}); g is the acceleration due to gravity; h_b is the bed elevation; and H is the ice thickness. The flotation criterion, F , is the ratio of non-local, subglacial water pressure, P_w , to the ice-overburden pressure, P_i ($F = P_w/P_i$). In reality F varies both in space and time according to the configuration of the drainage system, basal ice temperature, ice-overburden pressure and the underlying geology (Clarke, 2005). However, limited borehole observations from contemporary ice masses suggest subglacial water pressure is close to the ice-overburden pressure ($F > 0.95$, e.g. Kamb, 2001) so we assume $F \approx 1$ ($P_w = P_i$). Implicit in this assumption is that the bed was wholly warm-based and that basal melting and effective pressure were uniform. As meltwater should follow the maximum gradient of the hydraulic potential surface, simple routing mechanisms in ArcGIS were used to simulate meltwater drainage pathways and to identify hydraulic minima where water may have ponded (see Evatt et al., 2006; Siegert et al., 2007; Wright et al., 2008; Livingstone et al., 2013). To test the sensitivity of subglacial lakes and meltwater pathways to the parameter F we also used a value of 0.75 ($P_w/P_i = 0.75$).

The bed topography and seafloor bathymetry were derived from Gebco_08 data, a continuous DEM for ocean and land with a spatial resolution of 30 arc-seconds. High-resolution bathymetry data of the Great Lakes were manually added (NOAA National Geophysical Data Centre, U.S. Great Lakes Bathymetry) and the DEM was then re-gridded to 5 km cell size. Given that specific ice-surface and bed topographies are only known from modelled outputs, and thus contain significant uncertainty, we utilised many such outputs (Table 1) to examine where on the bed subglacial lakes and water drainage pathways were likely to have occurred. This includes numerical ice-sheet model data of palaeo-ice and -bed topographies from: ICE-5G (Peltier, 2004); CLIMAP (CLIMAP Project Members, 1984); GRISLI (from Álvarez-Solas et al., 2011); Glimmer-CISM (from Gregoire, 2010; Gregoire et al., 2012); and 3D-MUN Glacial Systems Model (GSM) (Tarasov et al., 2012) (see Table 1 for a summary). We also reconstructed the LGM NAIS from geological evidence (Dyke et al., 2002) by estimating ice-surface profiles along flow-lines and interpolating the data to form a 3D-surface elevation model. This was achieved using

$$h = C^{1/2} \quad (2)$$

where h is the parabolic ice-surface profile and C is a constant, which describes the overall stiffness of the flow. A value of three was chosen as a guide but with some editing of elevations so that the ice sheet resembled the multi-dome configuration reconstructed from geological evidence (Winsborrow, 2007). The ice surfaces were re-gridded at 5 km resolution and the current bed DEM corrected for isostasy using the modelled bed topography data (Fig. 1).

Most emphasis is given to 3D-MUN GSM as the model was calibrated against a large set of observational constraints, including relative sea-level data, present-day rates of surface uplift and a high resolution ice-marginal chronology derived from geological and geomorphological evidence (see Tarasov et al., 2012 and Table 1). Subglacial hydrological predictions were calculated for a sample of 10 higher probability model runs from the ensemble-based analyses of the NAIS using 3D-MUN GSM (see Tarasov et al., 2012). Basal melt rates enabled cold-bedded regions of the bed (zero basal melt) to be masked out at each time-slice (Table 1).

Predictions were calculated at 1000-yr time-slices through the evolution of the ice sheet (see Table 1 for details). These predictions were then compiled for individual ice indices (i.e. single model runs) and across all models to give an indication of subglacial lake persistence and likelihood. The depths (m) of simulated subglacial lakes (L_D) were calculated, for $F = 1$, as follows:

$$L_D = (\Phi_F - \Phi) / (\rho_w g) \quad (3)$$

where Φ_F is the hydraulic potential surface at the bed surface plus the hydraulic potential of the lake. We assumed that all lakes filled to their hydraulic potential lip. Subglacial lake likelihood maps (as per Evatt et al., 2006) were calculated for each model (run), to illustrate the lake residence time and occurrence over the range of ice-sheet geometries associated with the modelled glacial cycle.

There are a number of limitations to predicting subglacial lakes and meltwater drainage networks using the method outlined above: (i) the simplistic treatment of basal conditions (see above); (ii) the DEM includes some post-glacial filling of the true subglacial bed; (iii) the coarse resolution of the models (which is especially problematic for the orographically complex Cordilleran and for resolving smaller ice streams); (iv) none of the models include dynamic coupling between the ice and subglacial meltwater, so ice-surface flattening above subglacial lakes is not accounted for; and (v) in reality some lakes do not form in hydraulic minima, such as those created by high geothermal heat fluxes or behind frozen margins (see Livingstone et al., 2012). These are not modelled here. Despite these issues, we can have confidence in our results as the errors associated with the

Table 1

Summary of the ice-sheet models used in this study for calculating 3D-hydraulic potential surfaces.

Reference	Data	Ice sheet model	Key characteristics	Time slices	Weighting
Tarasov et al. (2012)	Ice and bed topographies, and basal melting (thermal regime). 10 model runs	3D-MUN Glacial Systems Model <ul style="list-style-type: none"> • 3D thermomechanically coupled; • cell size: 1° longitude by 0.5° latitude; • shallow-ice approximation; • visco-elastic bedrock response; • fully-coupled surface drainer; • parameterized climate forcing; • surface mass balance and calving modules; • relative sea level solver. 	Bayesian calibration of the model against a large set of observational constraints (including relative sea level data and high-resolution ice-margin chronology from geological and geomorphological data).	32–7 ka BP at 1 ka slices	1.0
Gregoire, (2010)	Ice and bed topographies	Glimmer-CISM <ul style="list-style-type: none"> • 3D thermomechanically coupled; • cell size: 40 km; • shallow-ice approximation; • all of ice is assumed lost once water depths reach > 500 m; • elastic crust–viscous mantle; • annual positive degree day model; • ice-sheet forced with monthly mean precipitation and monthly mean surface temperatures from FAMOUS 	Good agreement with LGM ice extent. The rate of deglaciation is also a good fit with the reconstruction from Dyke et al. (2002).	30–20 ka BP at 5 ka slices; 20–8 ka BP at 1 ka slices	0.5
Álvarez-Solas et al. (2011)	Ice and bed topographies	GRISLI <ul style="list-style-type: none"> • 3D thermomechanically coupled ice-sheet-ice-shelf model (see Ritz et al., 2001); • cell size: 40 km; • shallow ice-approximation for grounded ice; • longitudinal stresses for ice-shelf/ice-stream flow; • climate forcing: Climber-3α climate model; • elastic lithosphere–relaxed asthenosphere bedrock response. 	Ice sheet at 18 kyr BP shows good fit with reconstructions in terms of volume and geographical distribution, and also ice stream locations.	20–6 ka BP at 1 ka slices	0.5
Peltier (2004)	Ice and bed topographies	ICE-5G <ul style="list-style-type: none"> • cell size: 1 degree; • geophysical ice load reconstruction of the deglacial history. 	Constrained by relative sea level data and also ice-marginal history catalogued in Dyke and Prest (1987).	LGM	0.1
CLIMAP (1984)	Ice and bed topographies	N/A	Constructed from geological data using realistic parabolic ice-surface profiles along flow lines and then interpolated across the ice sheet to achieve a 3D-ice surface.	LGM	0.1
Dyke and Prest (1987)	Ice topography	N/A	Constructed from geological data using realistic parabolic ice-surface profiles along flow lines and then interpolated across the ice sheet to achieve a 3D-ice surface. Isostasy calculated by assuming an earth response of $0.27 \times$ ice thickness.	LGM	0.1

calculations typically under-predict lake locations and therefore our results are seen as minimum predictions.

3. Results

3.1. Subglacial lakes

3.1.1. 3D-MUN GSM

Ensemble 3D-MUN GSM outputs simulate subglacial lakes at all time-slices, with a prevalence of lakes within the large over-deepened valleys and basins beneath the Cordilleran Ice Sheet (CIS) and also in Hudson Bay, the Canadian Arctic Archipelago,

Great Lakes and along the suture zone between the Laurentide and Cordilleran ice sheets (Fig. 2). Those areas where subglacial lakes formed during > 50% of all ice-sheet model geometries comprise 100,325 km² (Fig. 2a–c), and of this 74,575 km² are predicted to have been persistent for > 50% of the modelled ice-sheet history (32–6 ka BP). When F is lowered to 0.75 subglacial lakes are predicted to have occurred in far greater frequency and magnitude (674,800 km² area with > 50% chance of forming a subglacial lake), occupying nigh-on all the significant bed depressions in the landscape (Fig. 2d). In almost all cases subglacial lakes predicted to form for $F=1$ are also simulated with $F=0.75$. Thus, Fig. 2d effectively gives an upper bound on those depressions capable of hosting a subglacial lake.

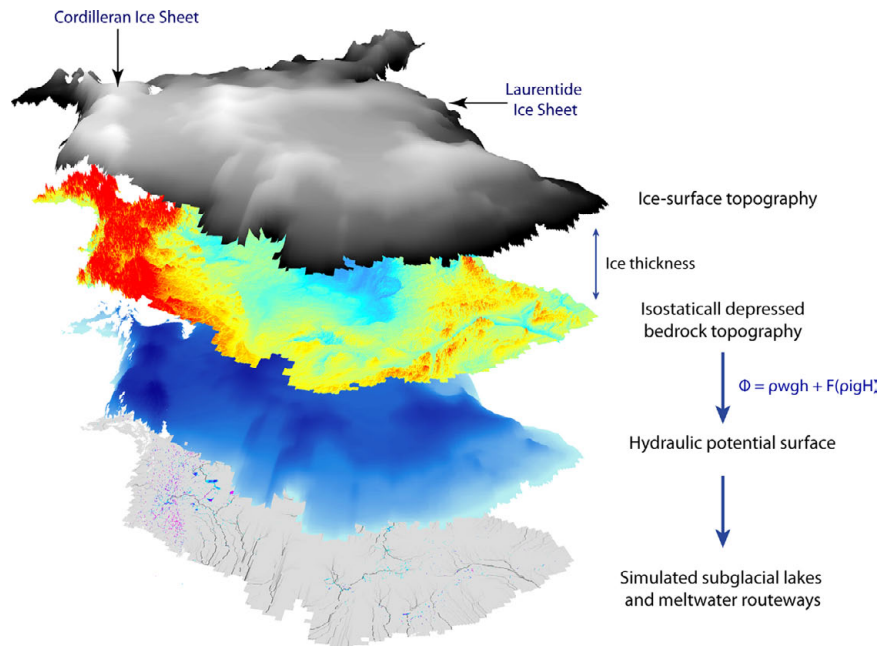


Fig. 1. Conceptual model detailing the generation of subglacial lake and meltwater drainage-pathway predictions. Digital Elevation Models of the bed topography and bathymetry (Gebco_08) and ice-surface and bed topographies from numerical ice-sheet models (Table 1) were used to calculate 5 km hydraulic potential surfaces of the North American Ice Sheet at discrete time-steps during the last glacial (Eq. (1)). Drainage pathways and subglacial lakes were then created with the hydrological tools in ArcGIS. Note, that isostatic depression derived from the models was added to the Gebco_08 DEM for each time slice. Note the North American Ice Sheet covered an area of ~16 million km² at its maximum (represented in this figure).

Fig. 3 demonstrates, for snapshots through one 3D-MUN GSM model run, how the locations of subglacial lakes changed as the ice- and bed-topographies evolved through the modelled glacial cycle. The results suggest spatial variability in lake persistence. Subglacial lakes in the Hudson Bay region are shown to be particularly transient, sensitive features, repeatedly forming and draining over time and changing locations (Figs. 2a and 3). These lakes are typically broad, shallow (up to ~10 m deep) features that can be visualised as lens-shaped. In contrast, those lakes beneath the CIS are typically small and deep (up to ~90 m) features that are able to persist throughout much of the last glacial (Figs. 2 and 3a).

During the latter stages of deglaciation (12–10 ka BP) very large (up to 250 km in diameter) subglacial lakes are predicted (Fig. 3). These are artefacts that form below large ice-surface depressions, caused by the formation of surface meltwater lakes. Surface lakes form in response to local ice-streaming - climate feedbacks. Whether these large surface lakes are physically-realistic is an open question (also see Marshall and Clarke 1999); in reality they may drain englacially or surficially before they get too big. Hence we do not include the hydrostatic load of the surface lakes in the modelling. Significantly, because water is denser than ice, the deeper centre of the lake will have a greater hydraulic potential than the margin and so subglacial meltwater may pond below the upstream portion and sides of the surface lake. If the bed is relatively flat a horseshoe-shaped subglacial lake will result (Fig. 5). This distinctive plan-form may allow ice-surface lakes to be validated or rejected based on the geological record of subglacial lakes.

As an additional experiment we used the modelled basal thermal regime (for 3D-MUN GSM) to investigate the effect on subglacial lake formation and distribution. This was achieved by masking out those regions where the model predicts cold-bedded conditions at each time-slice (see Fig. 4a for an example). In this scenario, the total area of those lakes that form during > 50% of all ice-sheet model geometries (32–6 ka BP) diminishes to 67,125 km²

(Fig. 4b and c). Of these lakes, those with > 90% chance of occurring are restricted to the CIS, suture zone between the Laurentide and Cordilleran ice sheets, and also within the onset zone of the Amundsen Gulf Palaeo-Ice Stream (Fig. 4c and d). This includes large lakes west of the Great Slave Lake, in the vicinity of Prince George City (British Columbia) and within the deep marine trench south of Victoria Island (Fig. 4c and d). Significant concentrations of high likelihood (> 50%) subglacial lakes also occur within, or at the onset zone of, more than 10 other palaeo-ice streams. This includes a sequence of lakes leading into Hudson Bay, those terrestrial ice streams associated with the Great Lake Ice Lobes (especially Lake Ontario) (Fig. 4b) and those draining northwards into the Arctic Ocean (Fig. 4d). Conversely, subglacial lake formation is shown to be scarce beneath some significant palaeo-ice streams, including M'Clure Strait, M'Clintock Channel and Cumberland Sound, and James and Des Moines lobes, both of which are terrestrially terminating (Fig. 4d).

3.1.2. All ice-sheet models

Likelihood maps calculated from all the available ice- and bed-topographies were weighted according to the quality and quantity of the modelled outputs (see Table 1). CLIMAP, ICE-5G and the Dyke et al. (2002) reconstructions were given the lowest weighting because they only generated predictions for the LGM time-slice. Conversely, the 3D-MUN GSM predictions (averaged over the 10 model runs) were given the greatest weighting because the model is calibrated to produce a good fit with the ice-marginal retreat history and relative sea-level data (Table 1).

Subglacial lake likelihood maps derived by combining the weighted maps from all individual model outputs typically reveal lower probabilities than for the 3D-MUN GSM dataset. Yet there is a similar spatial distribution to the predictions with lakes tending to occur beneath the CIS, and to a lesser extent along the suture zone between the Laurentide and Cordilleran ice sheets, the Great

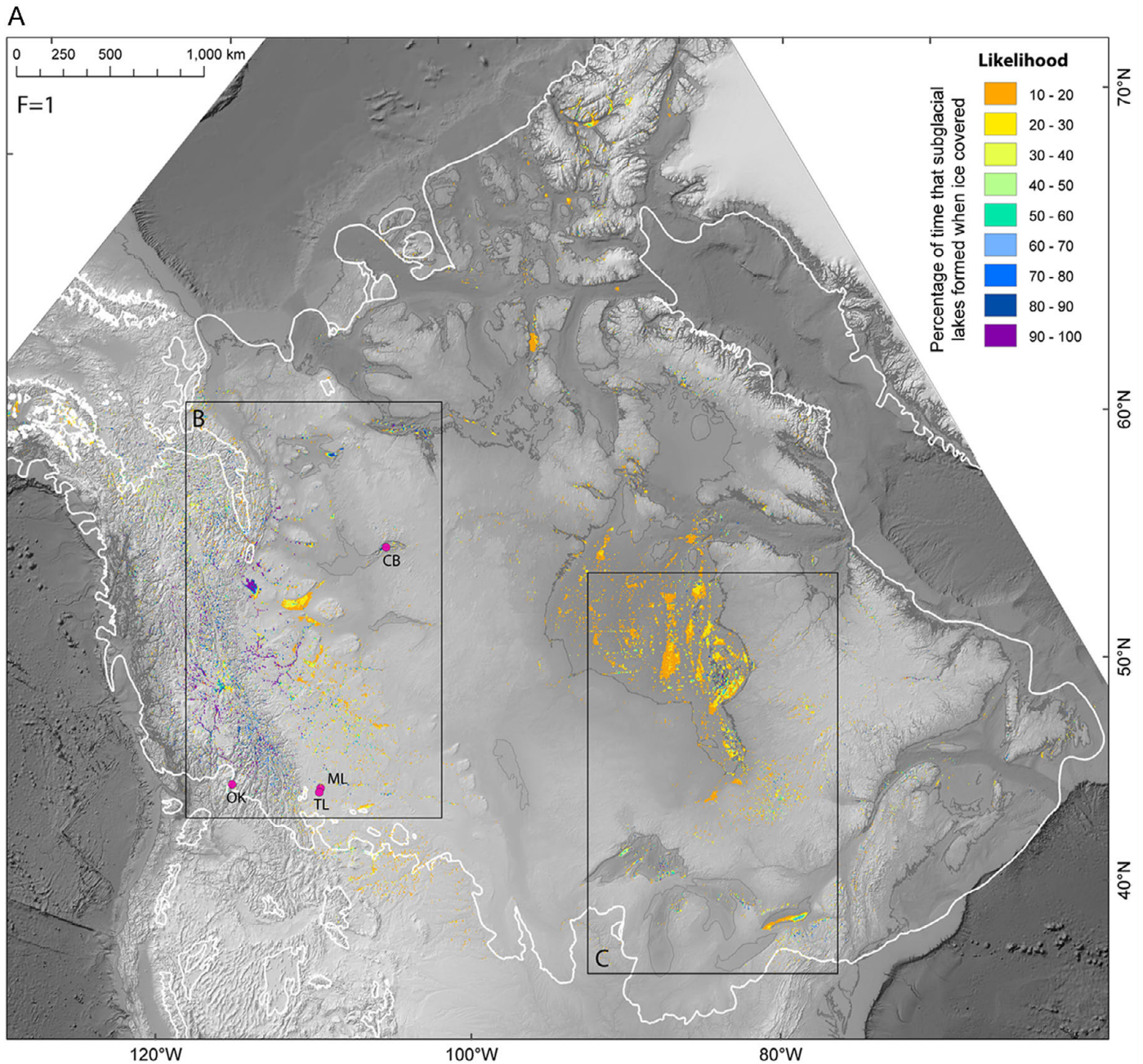


Fig. 2. Subglacial lake likelihood maps for the North American Ice Sheet from 32 to 6 ka BP using 3D MUN GSM. (A) Likelihood of a subglacial lake forming when $F=1$ (pink circles relate to published palaeo-subglacial lake records: CB: Christie Bay, Great Slave Lake; ML McGregor Lake; TL: Travers Lake; OK: Okanagan; white-line: LGM ice-margin); (B) close-up of the suture zone between the LIS and CIS (GBL: Great Bear Lake; GSL: Great Slave Lake; LL: Livingstone Lake); (C) close-up of the Great Lakes and Hudson Bay region of the LIS (JB: James Bay; LS: Lake Superior; GB: Green Bay; LM: Lake Michigan; LH: Lake Huron; GB: Georgian Bay; LE: Lake Eire; LO: Lake Ontario); and (D) likelihood of a subglacial lake forming with $F=0.75$. (For interpretation of the references to colour in this figure legend, the reader is referred to the web version of this article.)

Lake Basins, Hudson Bay and the Canadian Arctic archipelago (Fig. 5). In particular, more subglacial lakes are identified in the NE sector of the ice-sheet, through Hudson Bay and Strait and north-west of Baffin Island (Fig. 6). Those areas with $> 50\%$ chance of forming a subglacial lake span $42,125 \text{ km}^2$ (Fig. 6), and of this, $17,300 \text{ km}^2$ is predicted to be persistent for $> 50\%$ of the ice-sheet models evolution (32–6 ka BP, Fig. 6). Lowering the F -criterion to 0.75 results in significant ponding across large regions of the former ice-sheets bed, with a spatial distribution similar to that displayed in Fig. 2d. Those simulated subglacial lakes with $> 80\%$ likelihood are almost all located in CIS, with the exception of a few areas within Hudson Strait, Gulf of Boothia and Transition Bay palaeo-ice streams and the Great Slave Lake Basin (Fig. 6).

Fig. 7a indicates an exponential decline in subglacial lake area concomitant with a reduction in the extent of the NAIS ($R^2=0.84$). This is not a simple relationship as lake area is shown to vary considerably during time intervals when the ice sheet covered similar areas (e.g. between 14 and 16 million km^2 ; Fig. 7a). When the area is expressed as a percentage of the glaciated bed occupied by subglacial lakes a significant positive correlation is observed (Fig. 7b). Lake depth is integrated to estimate the total amount of meltwater stored beneath the last NAIS at each time-slice (Fig. 7c). This analysis suggests that during the LGM, $\sim 1000 \text{ km}^3$ of water (and possibly $\sim 3500 \text{ km}^3$) could have been impounded beneath the ice sheet, with this figure falling as the ice-sheet shrank post-LGM (Fig. 7c). However, there is evidence of considerable

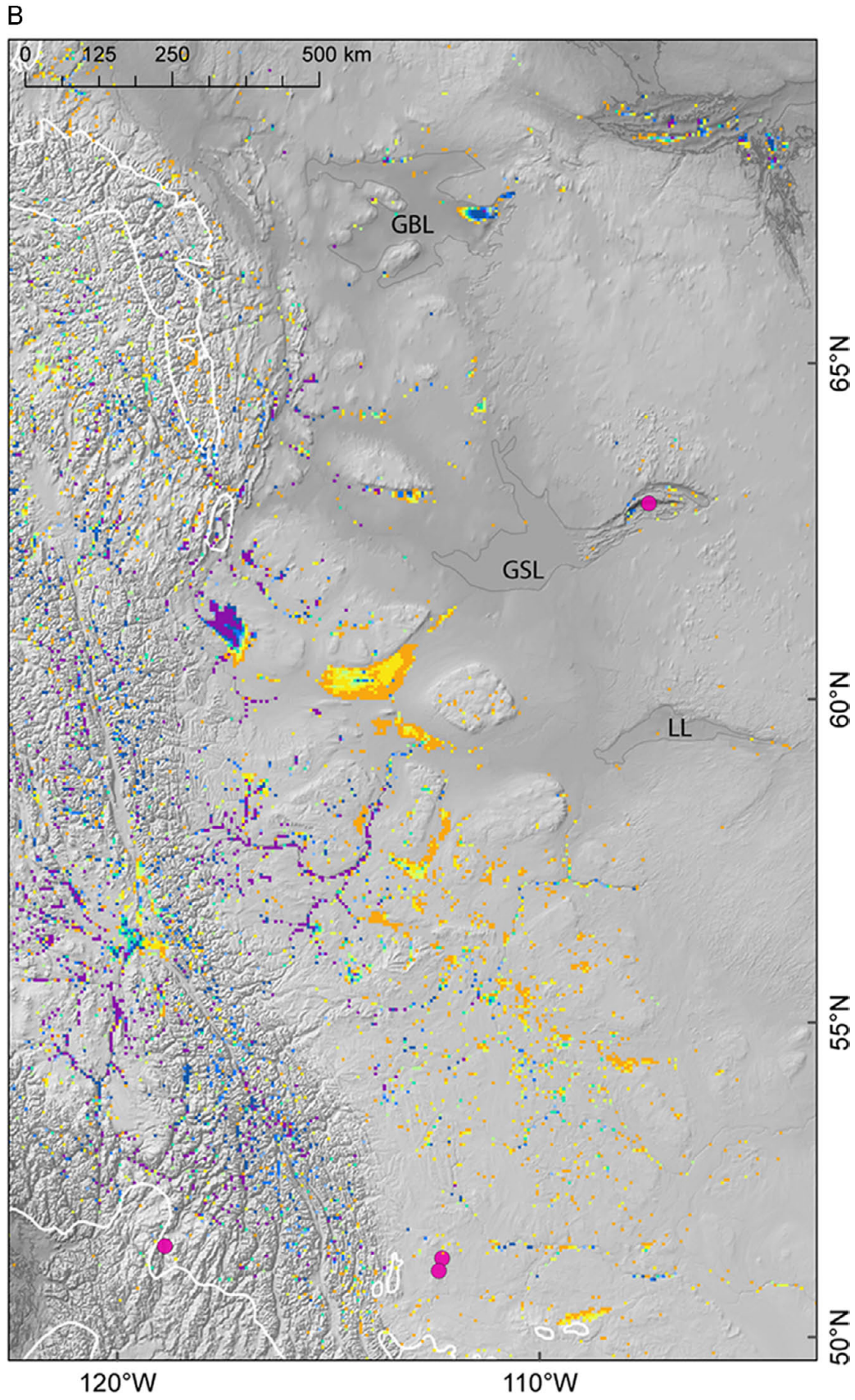


Fig. 2. Continued.

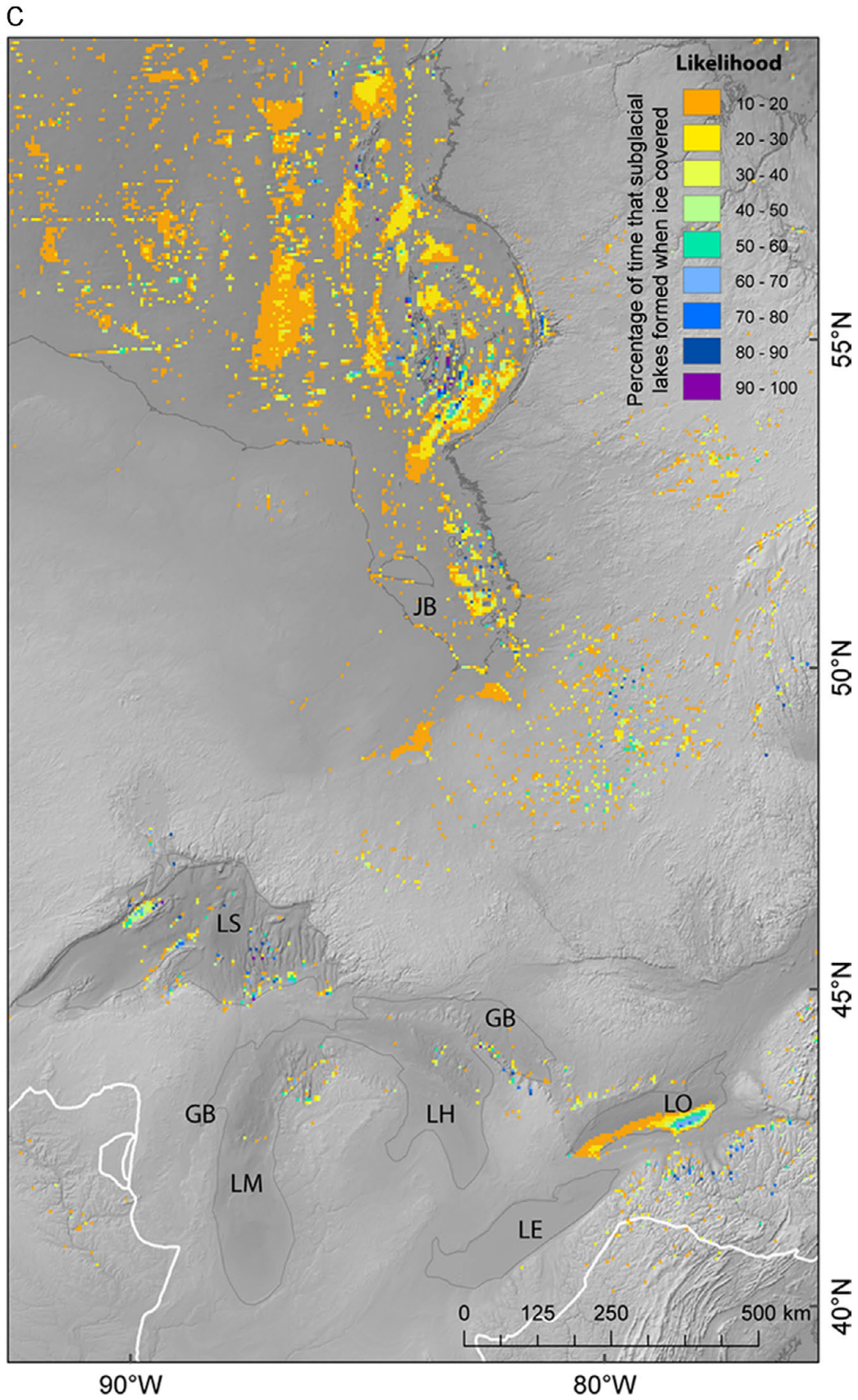


Fig. 2. Continued.

D

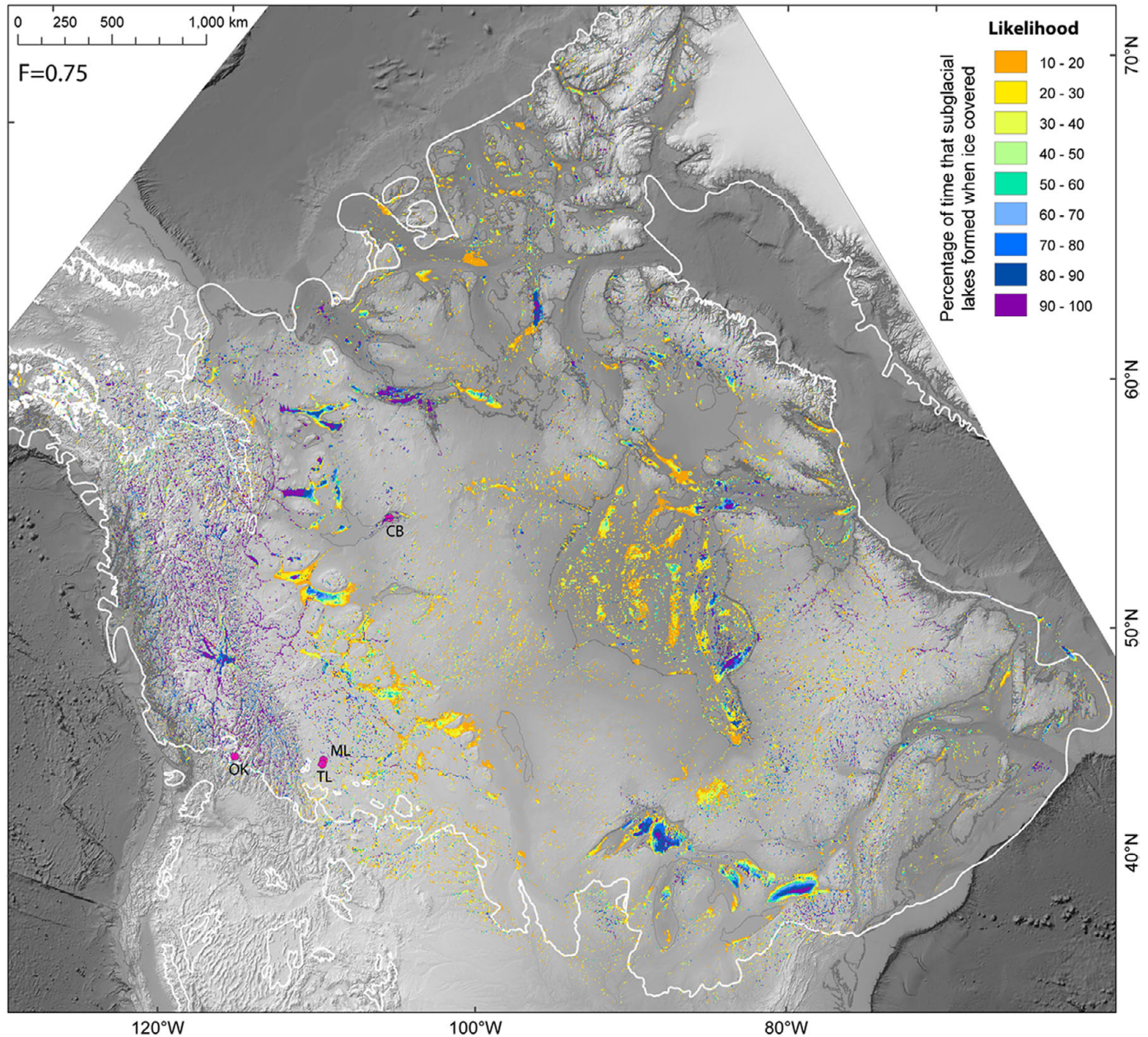


Fig. 2. Continued.

variability in water volumes, for example at ~18 ka BP (Fig. 7c). The typical hypsometry of lakes also varies, with lakes characteristically shallower and more extensive during ice expansion (e.g. 24–27 ka BP), and deep and small in area during the final stages of deglaciation (after ~16 ka BP).

3.2. Subglacial meltwater drainage-pathways

Simulated meltwater drainage beneath the NAIS is organised into a series of discrete catchments composed of dendritic pathways that flow roughly from the ice-sheet centre to the margin (Figs. 3 and 8). By far the greatest concentration of meltwater is through the Hudson Bay–Strait drainage network, although there are also significant systems draining into the Arctic Ocean and southwards along the suture zone between the CIS and LIS (Figs. 3 and 8). These large drainage networks are typically

associated with ice streams, including Hudson Strait, Amundsen Gulf, M'Clintock Channel, M'Clure Strait, Gulf of Boothia, Lancaster Sound, Cumberland Sound and the Gulf of Lawrence (Fig. 8).

Meltwater flow under some sectors of the NAIS is predicted to have been broadly stable, such as along the broad, deep trenches of the Canadian Arctic archipelago, through Hudson Strait and the Gulf of Lawrence and beneath the Lake Michigan Lobe (Fig. 8). In contrast, the suture zone between the Laurentide and Cordilleran ice sheets displays a convoluted drainage network, whilst Hudson Bay is characterised by a dendritic pattern (Figs. 3 and 8). Fig. 3 displays the evolution of the simulated subglacial drainage network (and predicted lakes) for one model run. Of particular note is the brief capture of the Hudson Bay drainage network at ~18 ka BP by the Cumberland Sound Palaeo-Ice Stream, before it switched back to re-occupy Hudson Strait by ~15 ka BP (Fig. 3). Moreover, the Glimmer-CISM model run (Gregoire, 2010) suggests

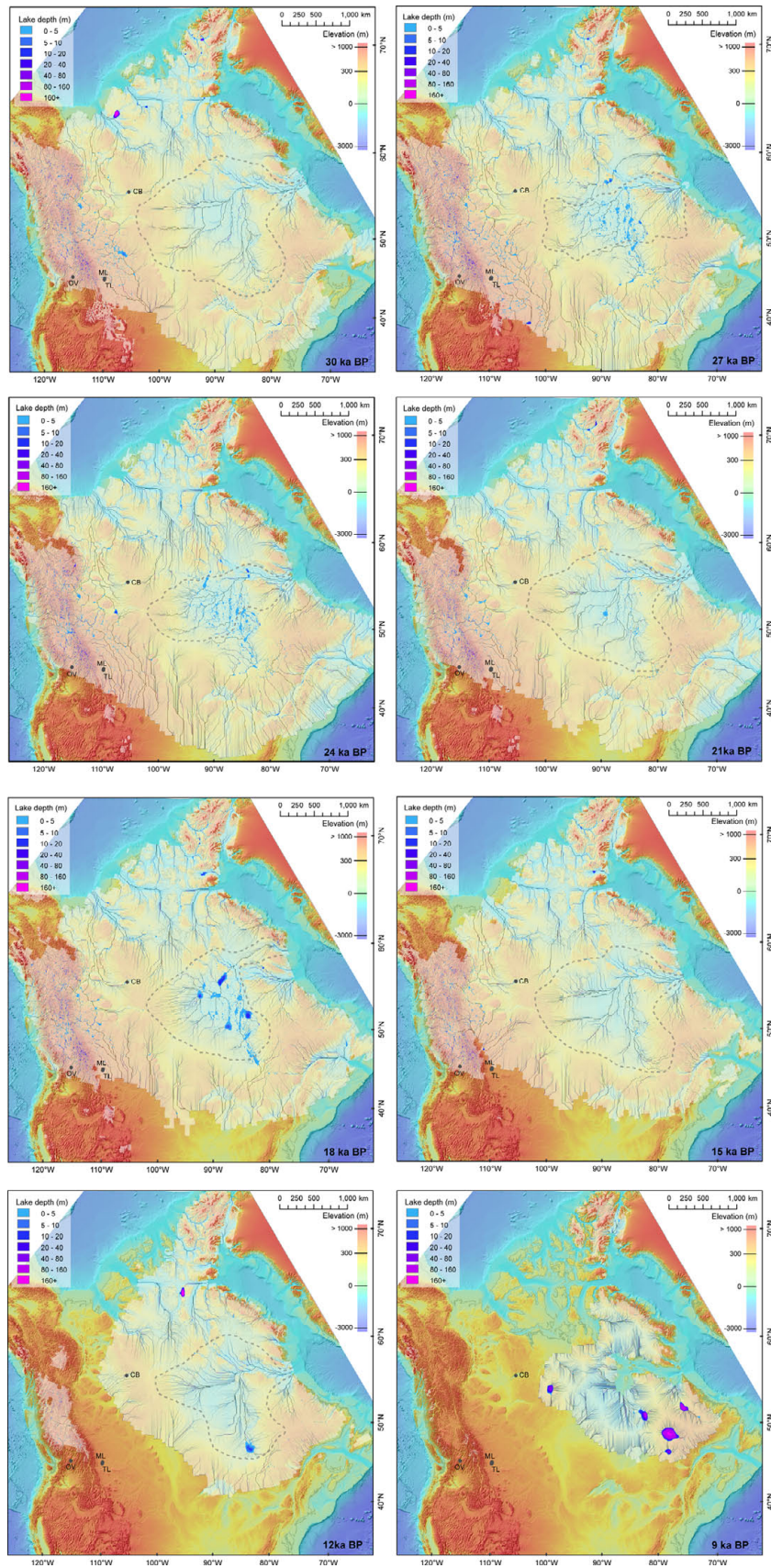


Fig. 3. Snapshots through one model run (LT9877) from 3D-MUN GSM showing the change in subglacial lake formation, lake depth and meltwater drainage pathways (darker lines indicate greater meltwater flow accumulation) at 30, 27, 24, 21, 18, 15, 12 and 9 ka BP (white opaque colour represents the modelled ice-sheet extent at each time-slice). Note the subglacial lake and drainage pathway fluctuations, especially in Hudson Bay (grey dotted line is the Hudson Bay drainage divide). The large lakes in the 9 and 12 ka BP timeslices are caused by depressions in the ice surface caused by supraglacial lakes. These supraglacial lakes are thought to form by local streaming and climate feedbacks (see text and Fig. 5 for more details about these features).

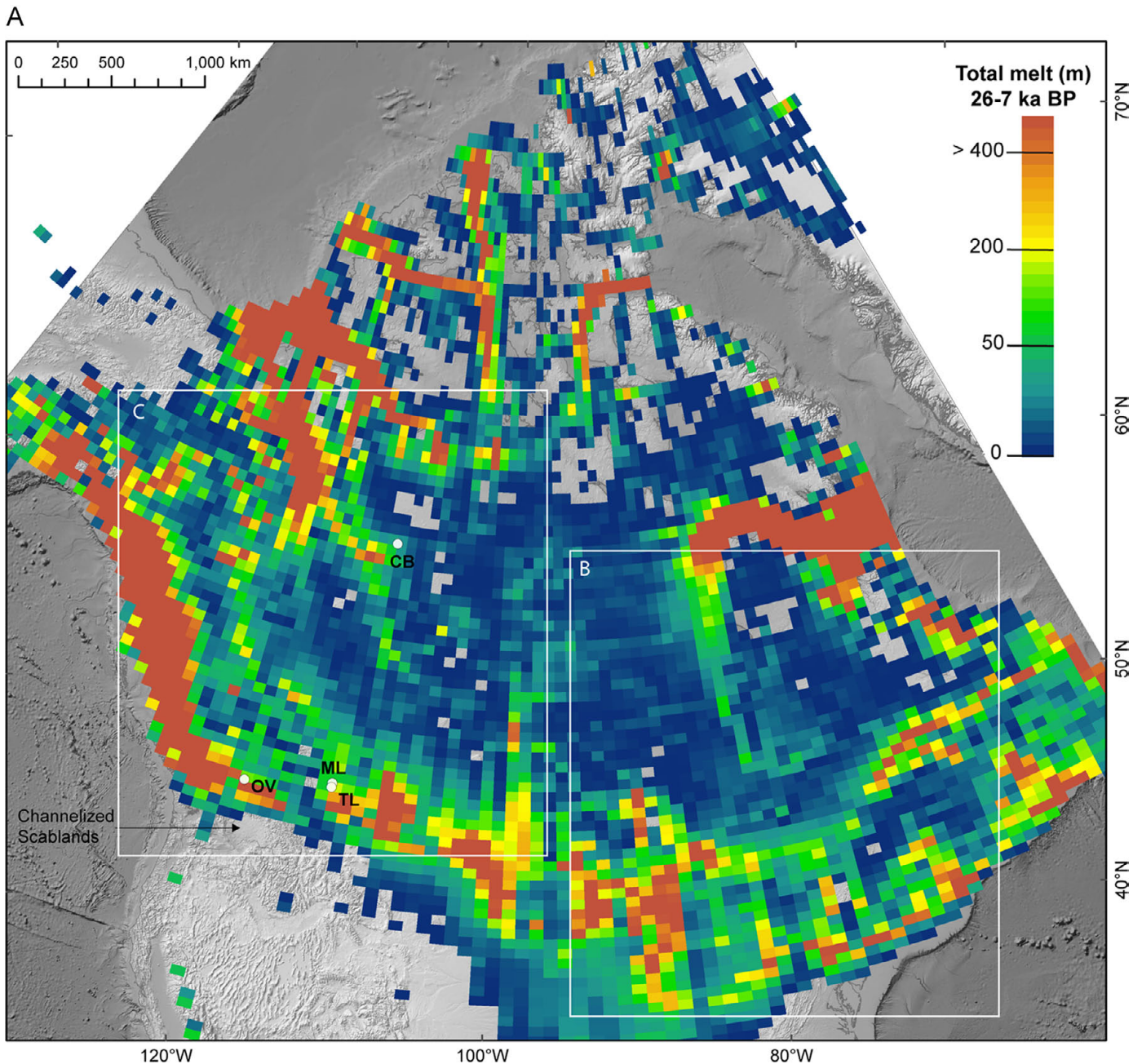


Fig. 4. (A) Total basal melt during the period 32–6 ka BP (from 3D-MUN GSM), averaged over the ten model runs, for $F=1$; (B) and (C) likelihood of a subglacial lakes forming beneath the eastern and western sectors of the former North American Ice Sheet between 32 and 6 ka BP using 3D-MUN GSM and with cold-bedded regions of the ice-sheet masked out at each time-step (see Fig. 2(B) and (C) for abbreviations. Dark pink arrows delineate the postulated pathway of the Livingstone Lake flood tract (e.g. Shaw, 1983)); and (D) significance map, whereby each point represents a pixel with > 50%, 80% and 90% chance of forming a subglacial lake and their association with palaeo-ice stream locations (from Winsborrow et al., 2004). Numbers refer to palaeo-ice streams (after Winsborrow et al., 2004): 1—Mackenzie; 2—Anderson; 3—Horton; 4—Haldane; 5—Great Bear; 6—Dubawnt Lake; 7—Saneraun Hills; 8—Collinson; 9—Flow set 76; 10—M’Clintock Channel; 11—Crooked Lake; 12—Transition Bay; 13—Peel Sound; 14—Central Alberta Ice Strea; 15—High Plains; 16, 17—Ungava Bay; 18—Amundsen Gulf; 19—M’Clure Strait; 20—Gulf of Boothia; 21—Admiralty Inlet; 22—Lancaster Sound; 23—Cumberland Sound; 24—Hudson Strait; 25—Gulf of St Lawrence; 26—Albany Bay; 27—Des Moines Lobe; 28—James Lobe; and 29—St Georges Bay. The white outlines in (B) and (C) delineate the LGM ice position. (For interpretation of the references to colour in this figure legend, the reader is referred to the web version of this article.)

repeated drainage switches between Hudson Bay–Strait and Hudson Bay–Gulf of Boothia, And the SW sector of the LIS also displays repeated adjustments to its drainage configuration (Fig. 3).

Simulated subglacial lakes are typically associated with major drainage routeways, often congregating towards ice-divides in the upper reaches of the network (Figs. 3 and 8). However, they are also found throughout the catchment as a series of lakes connected by meltwater routeways (Figs. 3 and 8). The exception is beneath the former CIS, where many of the subglacial lakes are in

locations independent of significant meltwater drainage paths (Fig. 3).

3.3. Glacial geomorphological evidence for palaeo-subglacial lakes and their drainage

Of the subglacial lakes identified in the literature, Great Slave Lake, which reaches up to 500 m below present-day sea-level (see Christoffersen et al., 2008), has a > 70% chance of occurring

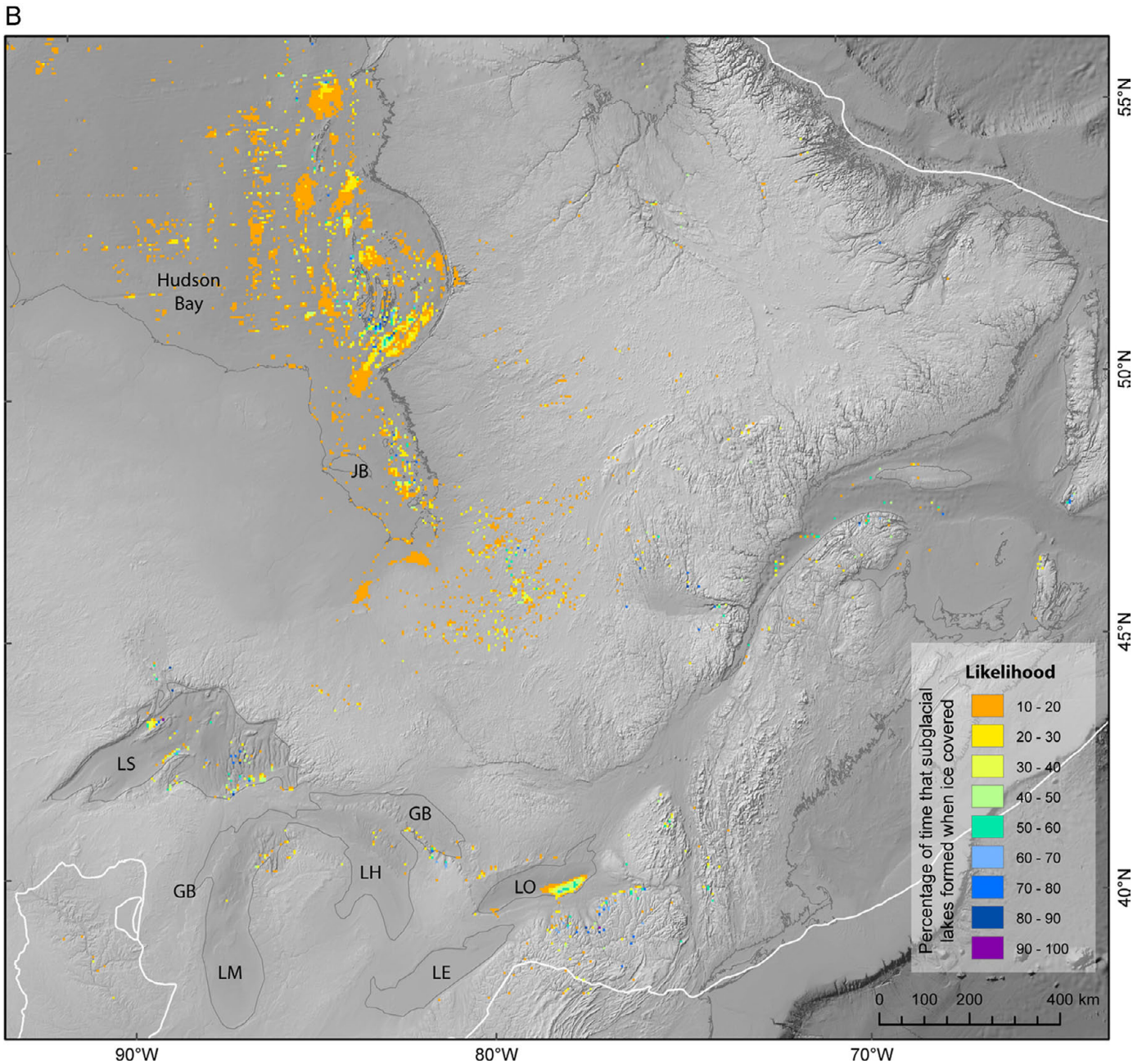


Fig. 4. Continued.

according to the results of our simulations (Figs. 2, 4 and 6). In contrast we predict that McGregor and Travers subglacial lakes (Munro-Stasiuk, 1999, 2003), in southern Alberta, have a <10% chance of forming. Subglacial lake Okanagan (Lesemann and Brennand, 2009), a 120 km long, 3–5 km wide glacially over-deepened bedrock trough that reaches up to 650 m below sea level, is not predicted using 3D-GSM MUN and has a <10% of forming when all the model runs are included. However, when recalculated using 3D-MUN GSM at higher resolution (1 km) and with the sediment fill (which is up to 800 m thick and interpreted to reflect focussed sediment deposition during the last glacial cycle: Eyles et al., 1991) removed a 50 m deep, persistent subglacial lake is predicted (Fig. 9). Moreover, a series of smaller, shallow subglacial lakes are simulated in the valley to the NE of Lake Okanagan, which would have preferentially drained into the main basin.

Shoemaker (1999) and Russell et al. (2003) proposed the formation of a subglacial lake in the Ontario Basin during the last glaciation. Saliiently, our modelling also predicts the formation of a persistent subglacial lake, ~70 km × 25 km and 13 m deep, along the SE margin of Lake Ontario during the last glacial (Fig. 10). Downstream of the simulated subglacial lake is the New York drumlin field which stretches some 40 km along the southern shoreline of Lake Ontario and extends ~40 km south to the New York Finger Lakes and the Appalachian Uplands. Glacial geomorphological mapping reveals that the New York drumlin field is dissected by a north-south system of meltwater channels (also see Muller and Cadwell, 1986; Petruccione et al., 1996) emanating from Lake Ontario and converging on the Finger Lakes (Fig. 10). The Finger Lakes themselves comprise eleven elongate basins that radiate out from the drumlin field, reaching up to 300 m below sea level and in-filled by up to 270 m of late Quaternary glacial

C

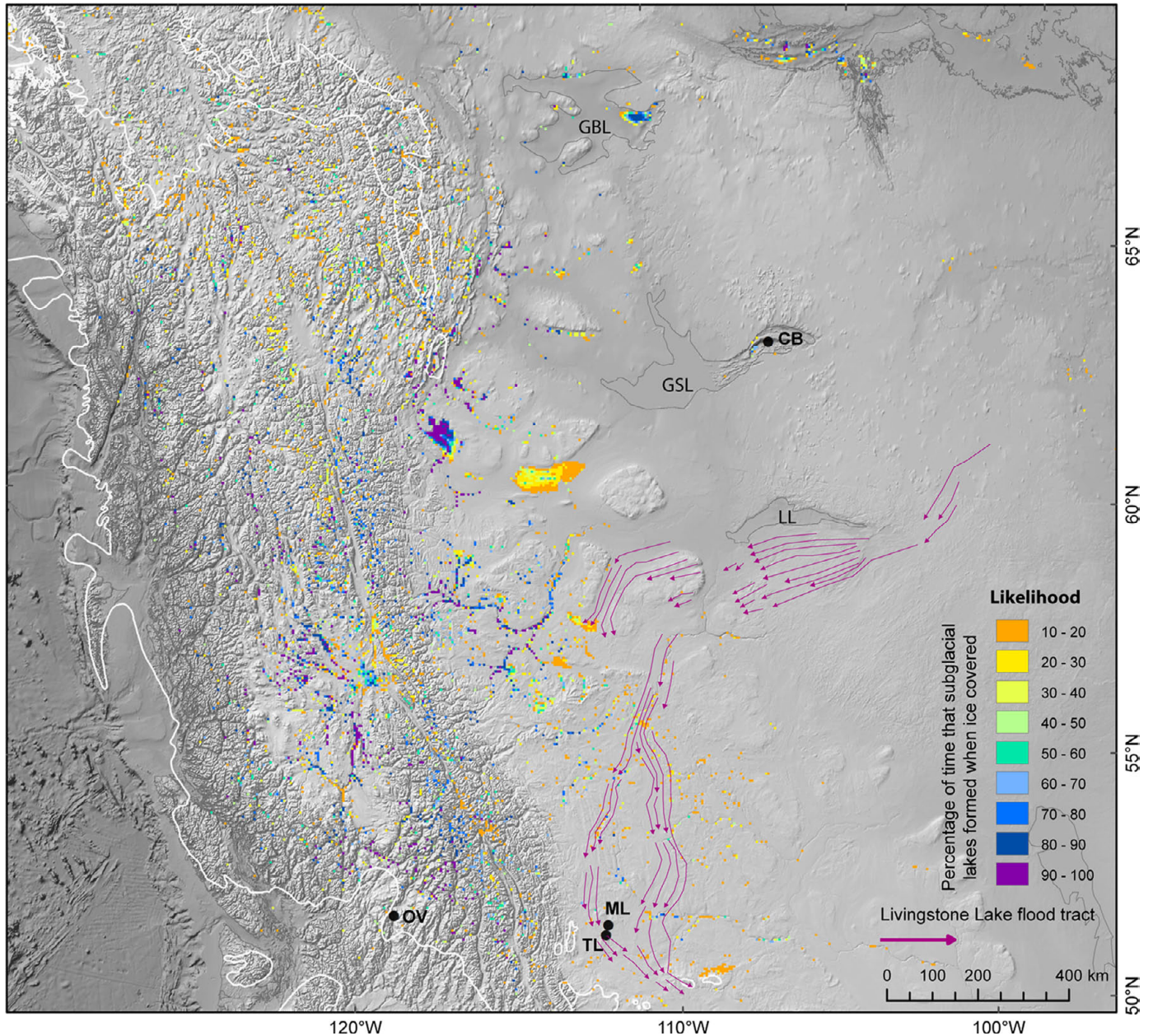


Fig. 4. Continued.

sediment (Mullins and Hinchey, 1989; Mullins et al., 1996). These overdeepened glacial basins are also predicted to have hosted subglacial lakes by our model (even without the late Quaternary sediment being stripped away) (Fig. 10).

The purported identification of extensive subglacial flood tracts beneath the former NAIS rests on the premise that glacial landforms observed along the flowpath (e.g. drumlins) were formed by meltwater (Shaw, 1983; Shaw and Kvill, 1984; Shaw et al., 1989; Shaw and Gilbert, 1990; Kor et al., 1991 and rebuttals by Clarke et al., 2005; Benn and Evans 2006; Evans et al., 2006, 2008). The most famous example is the Livingstone Lake drumlin event, which has been traced from the Northwest Territories, through northern Saskatchewan and much of Alberta into Montana (Fig. 4c). However, although large regions west of, and within, Hudson Bay reveal the possibility of subglacial lake formation the likelihood is typically low (< 10%) and the bed is thought to have been predominantly cold-bedded (Fig. 4).

4. Discussion

4.1. Simulated subglacial lakes and meltwater drainage channels

Results presented in this paper demonstrate the potential for subglacial lake genesis beneath the NAIS throughout the last glacial (also see Livingstone et al., 2012 for theoretical considerations). Similar to Antarctica (see Wright and Siegert, 2011), we predict a range of subglacial lake sizes, distributions (e.g. beneath ice streams, under ice-divides and along suture zones) and stabilities (Figs. 2–4, and 6). This includes a high-likelihood of up to 90 m deep subglacial lakes beneath the CIS in overdeepened basins and valleys, shallow (up to ~10 m, although typically shallower) lakes in Hudson Bay, and persistent subglacial lake formation in Lake Ontario, Georgian Bay, Great Bear Lake, Great Slave Lake and deep trenches of the Canadian Arctic Archipelago (Figs. 2–5). Subglacial lakes show a close correlation with a

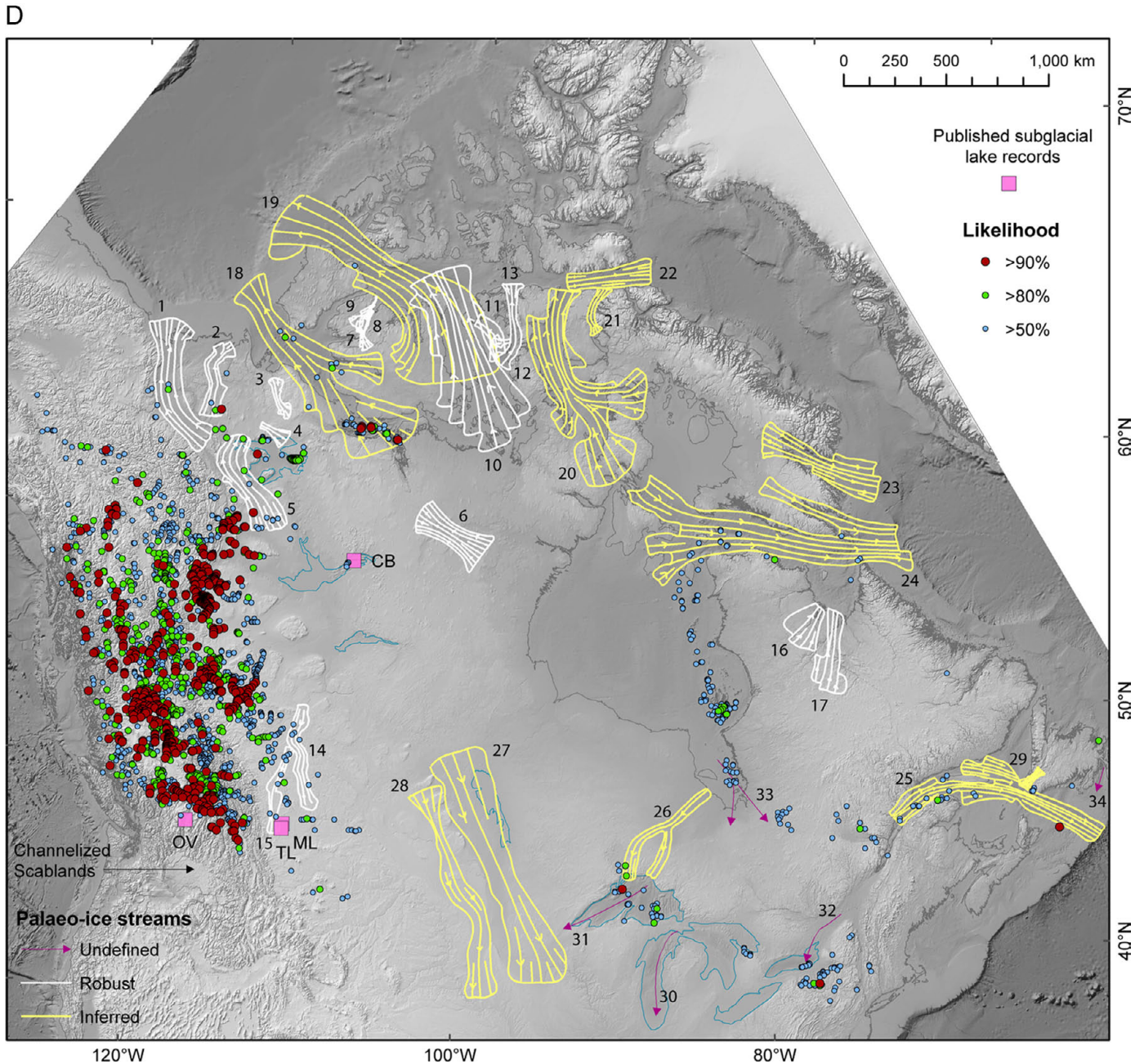


Fig. 4. Continued.

number of ice-streams, occurring both beneath onset zones (e.g. Amundsen Gulf Ice Stream) and along their length (e.g. Hudson Strait Ice Stream). This pattern is analogous to observations beneath Antarctica (e.g. Smith et al., 2009; Wright and Siegert, 2011), and is precipitated by lower ice-surface slopes relative to the surrounding ice-sheet (Figs. 3c and 6). Indeed, where subglacial lakes have been predicted in ice stream onset zones the lake occurrence may in part control (promote) the ice streams location. Significantly, similar distributions of predicted subglacial lakes are obtained irrespective of the model or model run, which suggests the results are robust.

Reducing the flotation criterion, F , results in significantly more subglacial lake predictions as the reduced influence of the ice-surface slope allows meltwater to be more readily trapped in depressions. Nevertheless, if subglacial lakes occupied the majority of depressions in the landscape the process of glacial

overdeepening is more difficult to explain. This implies that $F=0.75$ is an unrealistic value. However, it does highlight, how when ice-overburden pressure drops, such as towards the ice margin (i.e. open-channel flow and reduced ice thickness), localised subglacial ponding may become increasingly important. Furthermore, those few regions of the bed where subglacial lakes form for $F=1$ but not $F=0.75$ may provide interesting fieldwork locations as the bed topography has little influence on ponding, and therefore can occur in odd topographic settings (Livingstone et al., 2012).

The high frequency and persistence of subglacial lake predictions beneath the CIS, as easily inferred on the basis of elongated, glacially overdeepened valleys, make it a prime candidate for palaeo-subglacial lake investigations. Moreover, the Cordillera is characterised by high geothermal heat fluxes (Blackwell and Richards, 2004) and is therefore able to generate large volumes

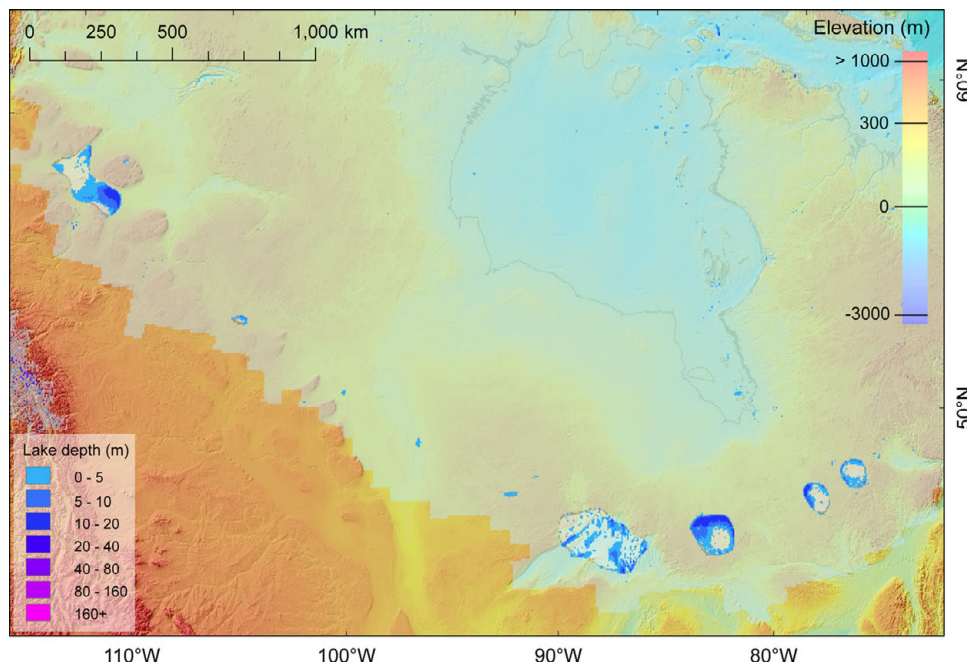


Fig. 5. Effect of large supraglacial lakes on subglacial lake formation when their hydrostatic load is taken into account. This figure is of the 14 ka BP time-slice (opaque blue colour delimits the ice-sheet extent). The faint grey outline around the large lakes illustrates the extent of the surface lakes. Note the horseshoe shape of the three most easterly lakes. In contrast the large subglacial lakes to the NW and in the Lake Superior basin do not mimic this shape because the topography also has a strong influence in these regions (i.e. rugged relief). (For interpretation of the references to colour in this figure legend, the reader is referred to the web version of this article.)

of meltwater at the ice-sheet bed. And, marine sedimentary evidence for repeated discharge of large volumes of freshwater and sediment into the Pacific Ocean during the advance and retreat of the CIS hints at the potential for subglacial outbursts of stored meltwaters (Lopes and Mix, 2009). The palaeo-bed itself is criss-crossed by meltwater channels (e.g. Lesemann and Brennand, 2009; Margold et al., 2011, 2013; Burke et al., 2012) and characterised by overdeepened valleys and basins (e.g. Eyles et al., 1991; Eyles and Mullins, 1997), blanketed by thick infills of Quaternary deposits (up to 800 m or more in depth), including complex sequences of glaciolacustrine, glaciofluvial and till facies, often dominated by ice-contact debris and other sediment gravity flows (e.g. Clague, 1975, 1988, 2000; Fulton and Smith, 1978; Eyles, 1987; Eyles and Clague, 1991; Lian and Hicock, 2001). Could some of these sequences, which have previously been interpreted to indicate repeated proglacial glaciolacustrine deposition during advance and retreat of the CIS, actually be diagnostic of palaeo-subglacial lake sedimentation? Or has much of the sediment fill been reworked and exported as till?

The flat-bed of Hudson Bay is predicted to comprise large, shallow subglacial lakes and broad, dendritic meltwater flow characterised by repeated drainage switches and events (Figs. 2–5, and 7). This environment is envisaged as water saturated sediments (e.g. fuzzy lakes, Carter et al., 2007). The repeated formation and drainage of very shallow but extensive subglacial lakes beneath Hudson Bay (see Fig. 3) is intimately related to the behaviour of Hudson Strait Palaeo-Ice Stream. When the ice stream was active and flowing rapidly (e.g. 30, 21 and 15 ka BP) ice was drawn-down from the surrounding onset zone. This caused the head of the ice-stream in Hudson Bay to steepen while the main trunk flattened out, inhibiting lake genesis and promoting drainage in the upper reaches of the catchment. Conversely, during quiescent phases (e.g. 27, 24 and 18 ka BP) ice built up in a reservoir area at the head of the ice stream, causing it to flatten out and subglacial lakes to form. Although 3D-MUN GSM uses the shallow-ice approximation and therefore does not capture the underlying mechanics of ice streams particularly well, the result still demonstrates the inherent

sensitivity of this sector of the ice sheet to shifts in ice-surface geometry, e.g. to binge–purge cycles (MacAyeal, 1993). In this example, water is stored in the onset zone during the binge phase and then driven out during the purge phase. Marine geophysical data reveals a thin (< 5 m) veneer of till, which has been moulded into glacial lineations, flutes, and de Geer moraines, and also subglacial channels incised through till and bedrock and sandy bedforms interpreted as mega-ripples (Josenhans and Zevenhuizen, 1990; Ross et al., 2011). The formation of glacial landforms in Hudson Bay confirms that the bed was wet at some-point during the last glacial, whilst high energy meltwater drainage is implied by the incised channels, and mega-ripples, which are diagnostic of mega-flooding (e.g. Bretz et al., 1956; Carling, 1996). Whether these landforms relate to subglacial and/or proglacial outburst floods, or constant drainage we can only speculate.

Fig. 7 reveals a drop in subglacial lakes concomitant with NAIS extent, and a reduced tendency to form as the ice shrank. Subglacial lakes are therefore predicted to have occupied their greatest extent and been most significant at the LGM. The reduced proclivity for subglacial lake formation through deglaciation is pertinent for investigating how meltwater drains (and is stored) at the bed and also the influence of subglacial lakes on ice-stream genesis(?) and stability (e.g. Bell et al., 2007; Stearns et al., 2008). One caveat is ice-surface flattening as a consequence of underlying subglacial lakes can help reinforce subglacial lake stability, which may override the reduced importance of subglacial lakes concomitant with a dwindling ice-sheet (see Livingstone et al., 2013).

At the LGM ~1000 km³ (and up to 3500 km³) of meltwater is simulated to be impounded beneath the NAIS, with this figure falling as the ice-sheet waned (Fig. 7c). The large variations in water volume relate to repeated formation (e.g. at 18 ka BP, Fig. 3) and drainage of large, shallow subglacial lakes in the Hudson Basin (see above). The proclivity towards smaller, deeper lakes during the later stages of deglaciation (Fig. 7c) is not surprising given that deep lakes are more stable than broad, shallow lakes. The total volumes are significantly lower than the 9000–16,000 km³

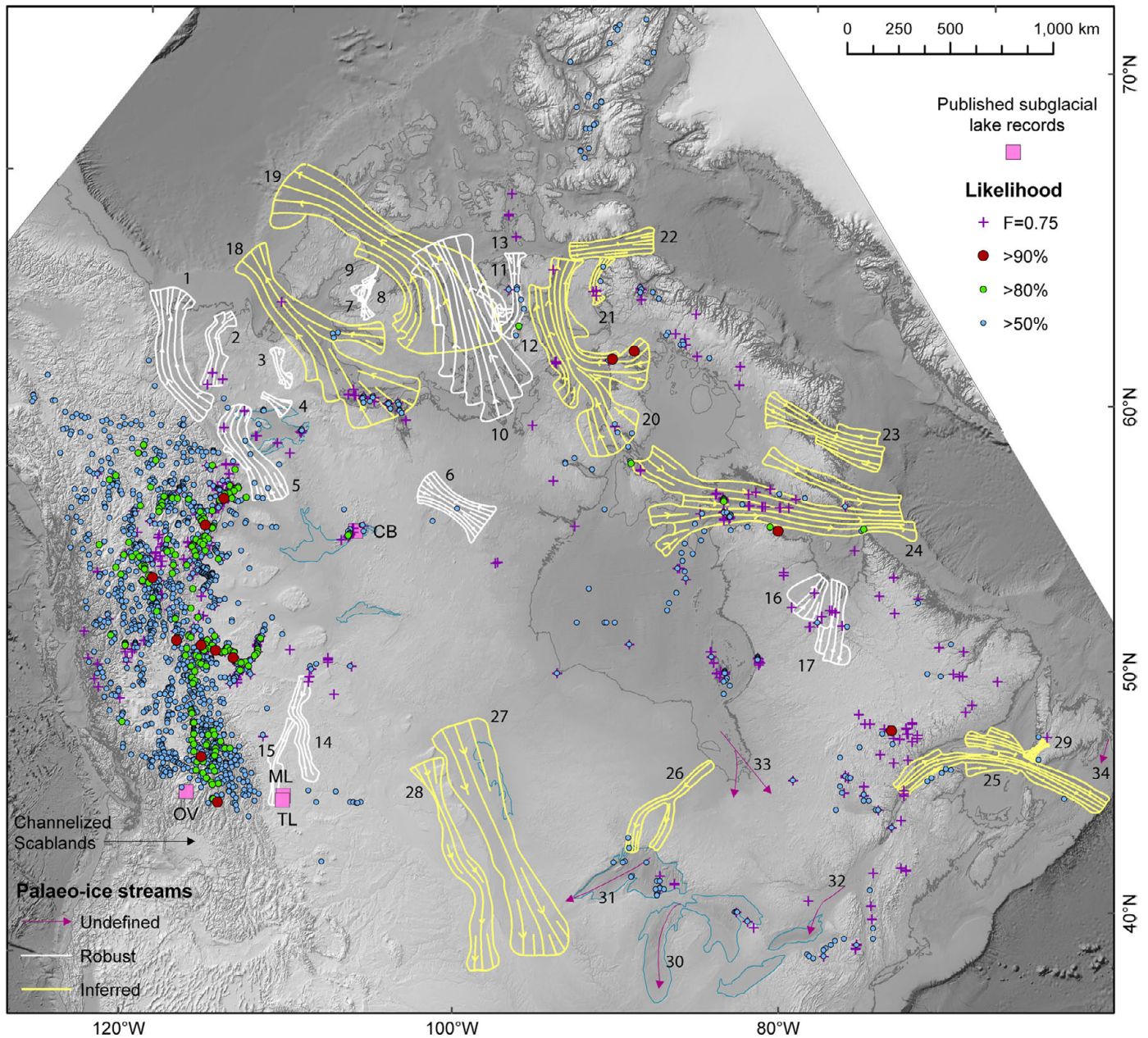


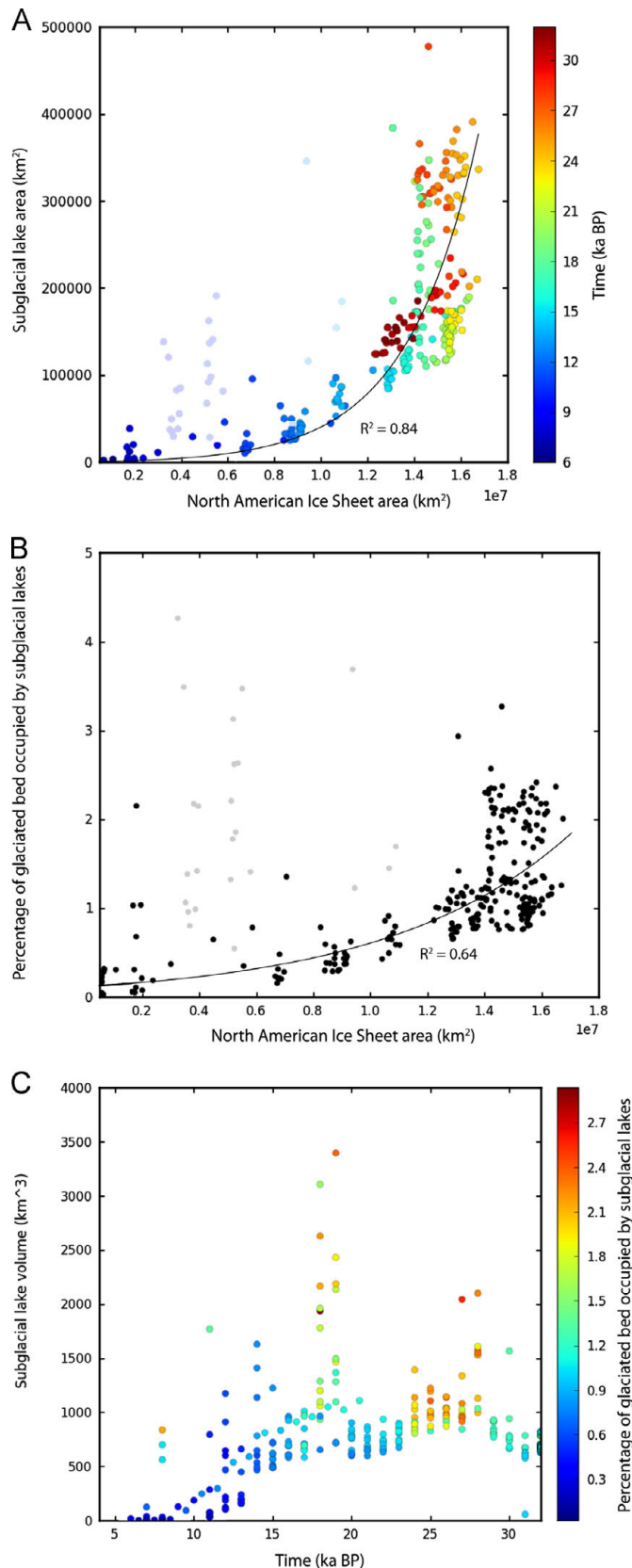
Fig. 6. Subglacial lake significance map for the NAIS from 32 to 6 ka BP compiled from all ice-sheet models and weighted according to Table 1. Each point represents a pixel with > 50%, 80% and 90% chance of forming a subglacial lake (and 95% chance for $F=0.75$) and their association with palaeo-ice stream locations. Numbers refer to named palaeo-ice streams (after Winsborrow et al., 2004; see Fig. 4C).

estimated to reside beneath the contemporary AIS (Wright and Siegert, 2011). However, a significant proportion of this meltwater (5400 km^3) is contained within the anomalously large Glacial-Lake Vostok. Moreover, the average depths used to calculate lake volumes in Antarctica (50–250 m) are significantly greater than those simulated beneath the NAIS (typically 3–6 m deep on average, with an upper range of ~95 m). This difference may arise because dynamic coupling between the ice and subglacial meltwater are not considered in our modelling. The ice-surface flattening feedback would (i) further lower the hydraulic potential surface allowing the lake to deepen; and (ii) promote subglacial lake stability, enabling the lake to survive longer. Glacial and postglacial infilling of basins would further reduce the predicted values. We therefore suggest that our estimates are lower bounds; despite the assumption the bed was wholly warm-based.

It has been speculated that drainage of subglacial stored meltwater into the North Atlantic could perturb ocean circulation and

therefore drive Dansgaard–Oeschger (D–O) events (Evatt et al., 2006). Models have shown that a freshwater influx of $< 0.1 \text{ Sv}$ ($1 \text{ sverdrup} = 1 \times 10^6 \text{ m}^3 \text{ s}^{-1}$) over a century is enough to slow the production of North Atlantic Deep Water (Rahmstorf, 1995; Ganopolski and Rahmstorf, 2001). However, changes in subglacial-lake storage between modelled time-slices is typically $< 1000 \text{ km}^3$ (Fig. 7c), and even if we assume that the drainage could occur within 1 yr and somehow was all advected unmixed to the active sites of NADW formation this still equates to $< 0.03 \text{ Sv}$ (Tarasov and Peltier, 2005). It is therefore highly unlikely that meltwater drainage from subglacial lakes could account for the 1500-yr periodicity D–O events or have a major impact on the ocean, even if released quickly.

Simulated drainage networks indicate significant meltwater concentration beneath palaeo-ice streams (Fig. 8), although this result is a consequence of ice-surface lowering of the fast-flowing ice rather than by meltwater lubrication. Drainage is shown to



convoluted network symptomatic of a sensitive hydraulic system susceptible to multiple shifts in meltwater flow. This pattern is replicated in Hudson Bay, where the dendritic network (Figs. 3 and 8) hints at a distributed system comprising broad, unconstrained meltwater flow. Overlapping drainage networks (Fig. 8) denote sensitive, hydro-dynamic regions of the former ice sheet bed (e.g. the suture zone of the Cordilleran and Laurentide ice sheets) where major meltwater routeways have shifted between and captured neighbouring catchments meltwater sources.

4.2. Comparison with glacial geomorphological and sedimentological evidence

All likelihood maps reveal a high chance (> 70%) of persistent (up to ~70% of the modelled time-slices) subglacial lake formation in the north-eastern limb of Great Slave Lake (Christie Bay) (Figs. 2, 4, and 6). This supports the findings of Christoffersen et al., (2008), whom interpreted a 150 m-thick sequences of fine-grained infill separating ice-contact glaciogenic sediments and Holocene lake sediments as subglacial lake facies. In contrast, we are unable to reproduce the McGregor and Travers palaeo-subglacial lakes (Munro-Stasiuk, 1999, 2003) with any confidence. This could either imply erroneous identification of the glaciolacustrine sediments as subglacial deposits (see arguments by Evans et al. (2006) for proglacial deposition of the same laminated and stratified glacial sediments), or alternatively subglacial ponds below the 5 km-resolution of the predictions.

Although the initial predictions are not able to reproduce a subglacial lake in the Okanagan Basin (after Lesemann and Brennand, 2009), stripping out the thick (up to 800 m) infill of glaciogenic sediments does result in a 50 m deep, persistent and relatively large (8 × 3 km²) subglacial lake in the southern-sector of the basin (Fig. 9). Certainly, deep infills of glaciogenic sediments clogging up the valleys and basins of the Cordillera will lead to our model under-predicting the frequency, stability and spatial extent of subglacial lakes by reducing the basins relief. A thick (up to 460 m) basal facies, restricted to the southern basin of Lake Okanagan, and comprising coarse-grained outwash gravels and boulders, is interpreted to represent deposition of subglacial and submarginal meltwaters (Eyles et al., 1991). This was assumed to indicate rapid deposition of sediment into a proglacial lake during deglaciation, although an alternative hypothesis could be subglacial deposition into a lake trapped at the ice-bed interface. A similar coarse-grained basal facies has been identified in north Okanagan Basin and also Kalamalka Lake, which although not coeval with the predictions, lie up to 600 m below sea-level (Fig. 9; Mullins et al., 1996; Mullins et al. 1990; Vanderburgh and Roberts, 1996). Coincidentally, similar facies have also been observed in the Finger Lakes, New York (see below, Mullins and Hinchey, 1989) and overdeepened glacial basins thought to have hosted subglacial lakes in the Swiss Alps (e.g. Hsü and Kelts, 1984; Lister, 1984; Pugin, 1989).

Fig. 7. (A) Scatter graph (of all ice-sheet model predictions) showing the relationship between ice-sheet area (km²) and subglacial lake area (km²), colour-coded according to time (ka BP); (B) scatter plot showing the relationship between ice sheet extent and the percentage of the bed occupied by subglacial lakes (for all ice sheet predictions). The greyed out points in (A) and (B) are those time-slices from 3D-MUN GSM where large supraglacial lakes are created. (C) Scatter plot showing subglacial lake volume (km³) against time (ka BP) and colour-coded by the percentage of the bed occupied by subglacial lakes. Note differences in the percentage of the bed occupied by subglacial lakes for similar lake volumes. This gives an indication of the sort of lakes developing at each time-slice (low volume, high percentage=lens-shaped lakes; high volume, low percentage=small, deep lakes). (For interpretation of the references to colour in this figure legend, the reader is referred to the web version of this article.)

have been broadly stable where topography exerts a strong control, such as beneath ice streams in the Canadian Arctic Archipelago, Hudson Strait, Cumberland Sound and Gulf of Lawrence. In contrast, the relatively flat suture zone running between the Cordilleran and Laurentide ice sheets displays a

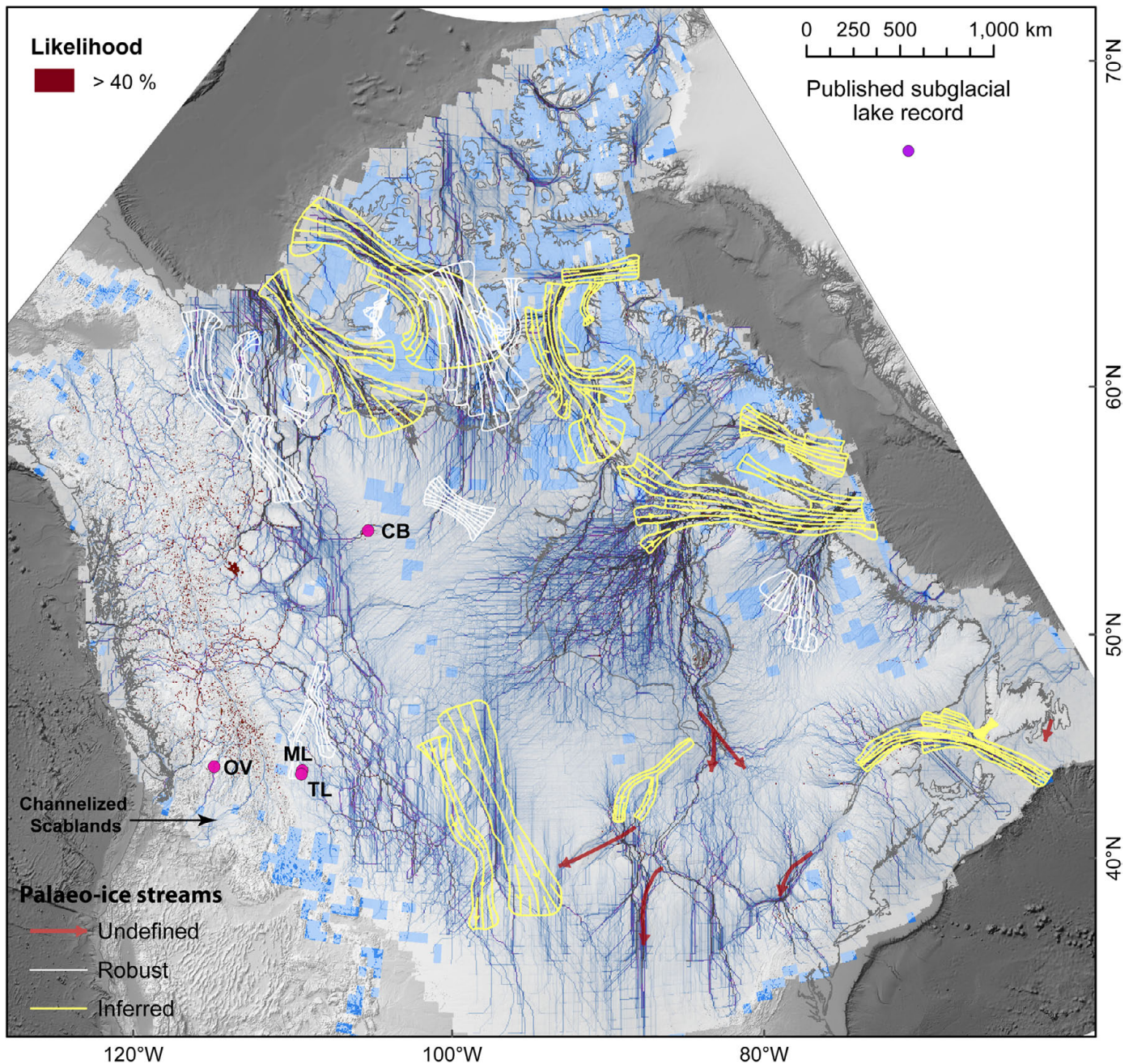


Fig. 8. Composite of all meltwater drainage predictions for all models and model runs (Table 1: 293 ice-surface geometries spanning a period of 32–6 ka BP) (blue, purple and then black lines represent an increase in meltwater drainage significance), ice-stream locations (after Winsborrow et al., 2004—numbers are the same as Fig. 4) and subglacial lakes with a > 40% chance of occurring. Note the drainage pathways do not differentiate between cold- and warm-bedded ice. Light blue colours denote those regions where 3D-MUN GSM predicts cold-bedded conditions throughout the last glacial for all 10 model runs used in the analysis. (For interpretation of the references to colour in this figure legend, the reader is referred to the web version of this article.)

The channelised scablands of the Columbia Plateau, Washington, has been interpreted as the result of cataclysmic flooding (Bretz, 1923) sourced by repeated outbursts from Glacial-Lake Missoula (e.g. Waitt, 1980, 1984). Recent modelling has cast some doubt on whether Glacial-Lake Missoula could have contributed all the meltwater needed to form the scablands (e.g. Miyamoto et al., 2007), lending credence to those advocating additional meltwater sources, such as from beneath the CIS (Shaw et al., 1999). However, this interpretation conflicts with accepted understanding of the field evidence (e.g. Atwater et al., 2000), while the latest 2D-modelling does not require further meltwater sources (Alho et al., 2010). Despite this, we infer that large volumes of meltwater were trapped beneath the CIS during the last glacial. And the Okanagan

Basin, which lies upstream of the channelised scablands, is a prime candidate for having hosted a subglacial lake (also see Lesemann and Brennand, 2009). Whether a subglacial lake could result in the sort of catastrophic flooding evinced by the channelised scablands remains unresolved.

Coincidence between the very large, persistent subglacial lake predicted in the Ontario Basin (as postulated by Shoemaker (1999) and Russell et al. (2003)) and the meltwater channels and New York Finger Lakes, which radiate out from it, is striking, and hints at a genetic association (Fig. 10). Indeed, the glacially overdeepened, elongate New York Finger Lakes are interpreted to have formed by localised subglacial meltwater erosion of pre-existing subglacially modified bedrock valleys (cf. Mullins and Hinchey,

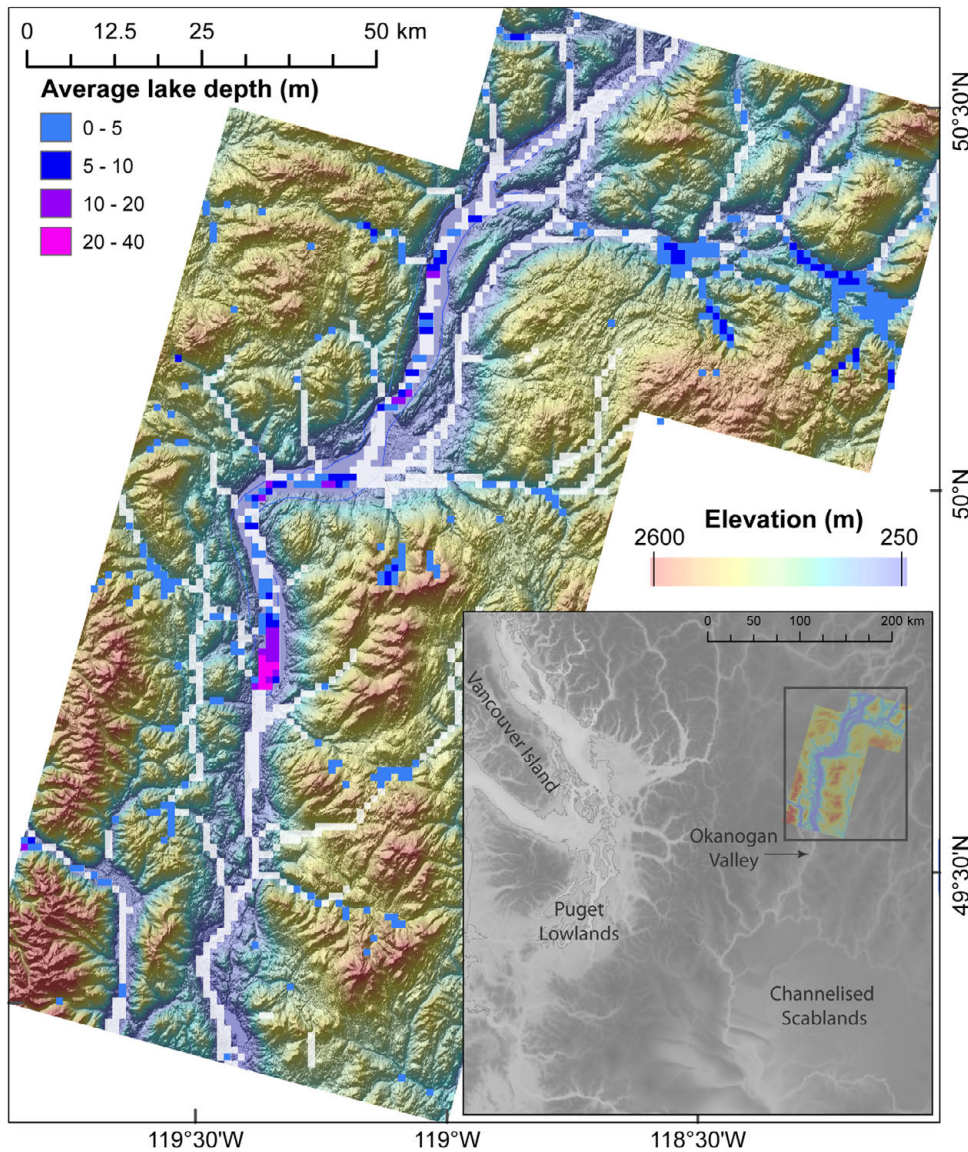


Fig. 9. Simulated drainage pathways (white lines) and subglacial lakes (at 1 km resolution) for the Okanogan catchment through the last glacial (32–15 ka BP) for one model run from 3D-MUN GSM. Average subglacial lake water depths for the Okanogan Basin and surrounding region, with the basins bathymetry included and Quaternary sediments stripped away. Significantly, a subglacial lake formed in the Okanogan basin during all time-slices, reaching a maximum of 50 m deep.

1989; Mullins et al., 1996; Pair, 1997). Significantly, the southern edge of the Finger Lakes contains a thick (up to 200 m) wedge of coarse-grained waterlain sand and gravel deposits, termed the Valley Heads moraine (Fig. 10; Mullins and Hinchey, 1989; Mullins et al., 1996). This facies is thought to have been deposited by subglacially pressurised meltwater (Mullins and Hinchey, 1989; Mullins et al., 1996) and is comparable to deposits observed in Lake Okanogan Basin. Thus, the postulated Subglacial Lake Ontario could have acted as a locus for focused downstream meltwater erosion during multiple drainage events, perhaps over multiple glaciations. Moreover, the complex pattern of small meltwater channels that coalesce towards the New York Finger Lakes implies meltwater (and sediment) concentration and downstream organisation. This fits with theory and observation, detailing sheet flow (in this case envisaged as a convolute network of small channels, Fig. 10) during the initial subglacial-lake dam-burst, followed by downstream evolution into large conduits as the flood quickly destabilises (Walder, 1982; Björnsson, 2002).

Finally, the lack of evidence for subglacial lake formation upstream of the Livingstone Lake drumlin field (Fig. 4c) questions the feasibility

of a subglacial meltwater origin, while the enormous volumes estimated to have produced the flood tract ($8.4 \times 10^4 \text{ km}^3$ —Shaw et al., 1989) are not reproducible in our modelling.

5. Conclusions

1. The subglacial hydrological modelling presented in this paper demonstrates the potential for subglacial lake formation beneath the North American Ice Sheet. Many subglacial lakes tend to occur beneath the CIS, along the suture zone between the Laurentide and Cordilleran ice sheets, in Hudson Bay, the Great Lake Basins and in the deep trenches of the Canadian Archipelago. This distribution is a robust result achieved irrespective of the model or model run used.
2. The simulated meltwater drainage network indicates significant meltwater concentration beneath palaeo-ice streams and varies between stable networks, typically associated with strong topographic controls (e.g. deep trenches in Canadian Arctic Archipelago) and convoluted networks characterised by

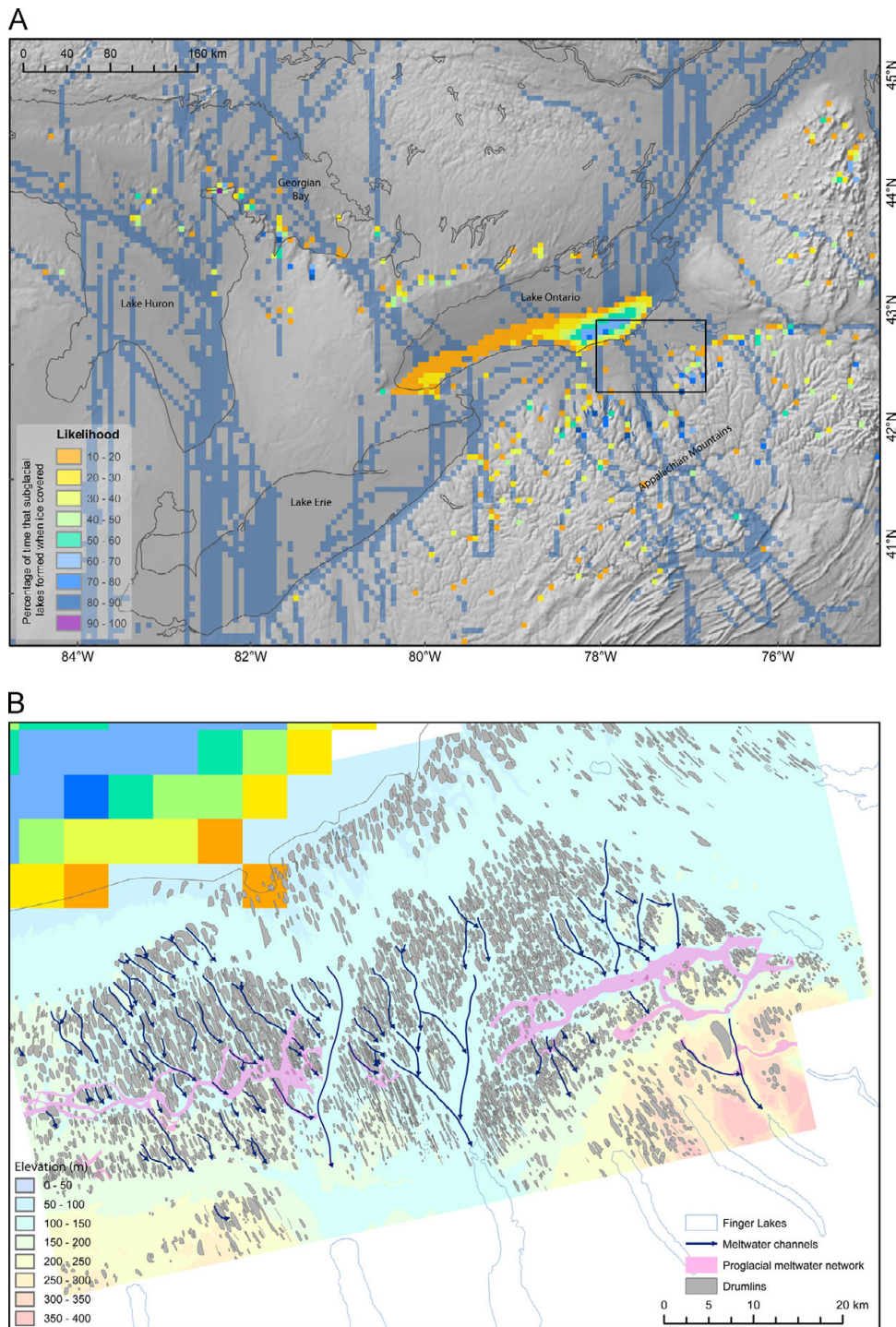


Fig. 10. (A) simulated meltwater routeway and subglacial lake predictions for the region surrounding Lake Ontario. The drainage routeways are a composite of all the models and model runs (see Fig. 7) and the subglacial lake predictions were derived from the 10 model runs of 3D-MUN GSM (Fig. 2a). (B) Glacial geomorphology map of the New York drumlin field on the southern shoreline of Lake Ontario. The landforms were mapped from a 10 m DEM (Cornell University Geospatial information repository). Channels were identified and classified according to the criteria of Greenwood et al. (2007). The 5 km pixels refer to the likelihood of subglacial lake formation in Lake Ontario (see (A)). Note the meltwater channels (dark blue arrows) at the downstream side of this high likelihood subglacial lake simulation, which cut through the drumlin field and converge towards the Finger Lakes. Also, note how the anastomosing course of the latterly formed proglacial meltwater channels has been conditioned by these NW-SE orientated meltwater channels. (For interpretation of the references to color in this figure legend, the reader is referred to the web version of this article.)

considerable hydro-dynamism (e.g. Hudson Bay, suture zone between the Cordilleran and Laurentide ice sheets). We also demonstrate the susceptibility of certain sites to meltwater capture by neighbouring drainage networks, best revealed by the repeated re-routing of the meltwater network from Hudson Bay into Hudson Strait and Gulf of Boothia.

3. We suggest these subglacial lake likelihood predictions could usefully form targets for detailed field and remote investigations. Preliminary action is taken by comparing purported palaeo-subglacial lakes and their meltwater drainage pathways with our predictions. Results reveal a strong tendency for subglacial lake formation in Okanagan Basin, Lake Ontario and Great Slave Lake,

but a limited chance of significant ($> 5 \text{ km}^2$) subglacial lake formation in McGregor or Travers basins. Moreover, we identify a possible palaeo-subglacial lake drainage network emanating from Lake Ontario. In contrast, the largely discredited 'mega-flood' tracts do not correspond to large upstream subglacial lakes.

Acknowledgements

This work was supported by a NERC Early Career Research Fellowship awarded to SJL (NE/H015256/1). We thank Lauren Gregoire and Jorge Álvarez-Solas for supplying numerical ice-sheet model output and Jonathon Kingslake for reading through and commenting on an earlier draft. This paper is a contribution to the INQUA sponsored project: "Meltwater routing and Ocean–Cryosphere–Atmosphere response" (MOCA). The paper has benefitted substantially from the insightful comments of two anonymous reviewers.

References

- Alho, P., Baker, V.R., Smith, L.N., 2010. Paleohydrological reconstruction of the largest Glacial Lake Missoula draining(s). *Quat. Sci. Rev.* 29, 3067–3078.
- Álvarez-Solas, J., Montoya, M., Ritz, C., Ramstein, G., Charbit, S., Dumas, C., Nisancioglu, K., Dokken, T., Ganopolski, A., 2011. Heinrich event 1: an example of dynamical ice-sheet reaction of oceanic changes. *Clim. Past* 7, 1297–1306.
- Atwater, B.F., Smith, G.A., Waitt, R.B., 2000. The channeled scablands: back to Bretz?: comment and reply comment. *Geology* 28, 574–576.
- Banerjee, I., McDonald, B.C., 1975. Nature of esker sedimentation. In: Jopling, A.V., McDonald, B.C. (Eds.), *Glaciofluvial and Glaciolacustrine Sedimentation*, vol. 23. SEPM Special Publication, Tulsa, OK, pp. 132–154. (497 pp.).
- Bartholomew, I., Nienow, P., Mair, D., Hubbard, A., King, M.A., Sole, A., 2010. Seasonal evolution of subglacial drainage and acceleration in a Greenland outlet glacier. *Nat. Geosci.* 3, 408–411, <http://dx.doi.org/10.1038/ngeo863>.
- Bell, R.E., Studinger, M., Shuman, C.A., Fahnestock, M.A., Joughin, I., 2007. Large subglacial lakes in East Antarctica at the onset of fast-flowing ice streams. *Nature* 445, 904–907.
- Benn, D.I., Evans, D.J.A., 2006. Subglacial megafloods: outrageous hypothesis or just outrageous?. In: Knight, P.G. (Ed.), *Glacier Science and Environmental Change*. Blackwell, Oxford, pp. 42–46.
- Blackwell, D.D., Richards, M., 2004. *Geothermal Map of North America*. American Association of Petroleum Geologists (AAPG), 1 sheet, Scale 1:6,500,000.
- Björnsson, H., 2002. Subglacial lakes and jökulhlups in Iceland. *Global Planet. Change* 35, 255–271.
- Bretz, J.H., 1923. The channelized scablands of the Colombia Plateau. *J. Geol.* 31, 617–649.
- Bretz, J.H., Smith, H.T.U., Neff, G.E., 1956. Channelized Scabland of Washington: new data and interpretations. *Geol. Soc. Am. Bull.* 67, 957–1049.
- Burke, M.J., Brennand, T.A., Perkins, A.J., 2012. Evolution of the subglacial hydrological system beneath the rapidly decaying Cordilleran Ice Sheet caused by ice-dammed lake drainage: implications for meltwater-induced acceleration. *Quat. Sci. Rev.* 50, 125–140.
- Carling, P.A., 1996. Morphology, sedimentology and palaeo-hydrological significance of large gravel dunes: Altai Mountains, Siberia. *Sedimentology* 43, 647–664.
- Carter, S.P., Blankenship, D.D., Peters, M.E., Young, D.A., Holt, J.W., Morse, D.L., 2007. Radar-based subglacial lake classification in Antarctica. *Geochem. Geophys. Geosyst.* 8, Q03016.
- Christoffersen, P., Tulaczyk, S., Wattrus, N.J., Peterson, J., Quintana-Krupinski, N., Clark, C.D., Sjunneskog, C., 2008. Large subglacial lake beneath the Laurentide Ice Sheet inferred from sedimentary sequences. *Geology* 36, 563–566.
- Clague, J.J., 1975. Late Quaternary sediments and geomorphic history of the southern Rocky Mountains Trench, British Columbia. *Can. J. Earth Sci.* 12, 595–605.
- Clague, J.J., 1988. Quaternary stratigraphy and history, Quesnel, British Columbia. *Géogr. Phys. Quat.* 42, 279–288.
- Clague, J.J., 2000. Recognizing order in chaotic sequences of Quaternary sediments in the Canadian Cordillera. *Quat. Int.*, 29–38.
- Clark, P.U., Walder, J.S., 1994. Subglacial drainage, eskers, and deforming beds beneath the Laurentide and Eurasian ice sheets. *Geol. Soc. Am. Bull.* 106, 304–314.
- Clarke, G.K.C., 2005. Subglacial processes. *Annu. Rev. Earth Planet. Sci.* 33, 247–276.
- Clarke, G.K.C., Leverington, D.W., Teller, J.T., Dyke, A.S., Marshall, S.J., 2005. Fresh arguments against the Shaw megaflood hypothesis: a reply to comments by David Sharpe on 'Paleohydrologics of the last outburst flood from glacial Lake Agassiz and the 8200 BP cold event'. *Quat. Sci. Rev.* 224, 1533–1541.
- CLIMAP Project Members, 1984. The last interglacial ocean. *Quat. Res.* 21, 123–224.
- Dyke, A.S., Prest, V.K., 1987. Late Wisconsin and Holocene history of the Laurentide Ice Sheet. *Géograph. Phys. Quat.* 41, 237–263.
- Dyke, A.S., Andrews, J.T., Clark, P.U., England, J.H., Miller, G.H., Shaw, J., Veillette, J.J., 2002. The Laurentide and Innuitian ice sheets during the Last Glacial Maximum. *Quat. Sci. Rev.* 21, 9–31.
- Engelhardt, H.F., Kamb, B., 1997. Basal hydraulic system of a West Antarctic ice stream: constraints from borehole observations. *J. Glaciol.* 43, 207–230.
- Evans, D.J.A., Rea, B.R., Hiemstra, J.F., Ó Cofaigh, C., 2006. A critical assessment of subglacial mega-floods: a case study of glacial sediments and landforms in south-central Alberta, Canada. *Quat. Sci. Rev.* 25, 1638–1667.
- Evans, D.J.A., Clark, C.D., Rea, B.R., 2008. Landform and sediment imprints of fast glacier flow in the southwest Laurentide Ice Sheet. *J. Quat. Sci.* 23, 249–272.
- Evatt, G.W., Fowler, A.C., Clark, C.D., Hulton, N.R.J., 2006. Subglacial floods beneath ice sheets. *Philos. Trans. R. Soc. London, Ser. A* 374, 1769–1794.
- Eyles, N., 1987. Late Pleistocene debris flow deposits in large ice contact lakes in British Columbia and Alaska. *Sediment. Geol.* 53, 33–71.
- Eyles, N., Clague, J.J., 1991. Glaciolacustrine sedimentation during advance and retreat of the Cordilleran ice sheet in central British Columbia. *Géogr. Phys. Quat.* 45, 317–331.
- Eyles, N., Mullins, H.T., Hine, A.C., 1991b. The seismic stratigraphy of Okanagan Lake, British Columbia: a record of rapid deglaciation in a deep 'fjord-lake' basin. *Sediment. Geol.* 73, 13–41.
- Eyles, N., Mullins, H.T., 1997. Seismic-stratigraphy of Shuswap Lake, British Columbia, Canada. *Sediment. Geol.* 109, 283–303.
- Fisher, T.G., Jol, H.M., Boudreau, A.M., 2005. Saignaw Lobe tunnel channels (Laurentide Ice Sheet) and their significance in south-central Michigan, USA. *Quat. Sci. Rev.* 24, 2375–2391.
- Fulton, R.J., Smith, G.W., 1978. Late Pleistocene stratigraphy of south-central British Columbia. *Can. J. Earth Sci.* 15, 971–980.
- Ganopolski, A., Rahmstorf, S., 2001. Rapid changes of glacial climate simulated in a coupled climate model. *Nature* 409, 153–158.
- Gjessing, J., 1960. Isavsmelningstidens drenering, dens forløp og formdannende virkning i Nordre Atnedalen med sammenlignende studier fra Nordre Gudbrandsdalen. *Ad Novas*.
- Gorrell, G., Shaw, J., 1991. Deposition in an esker, bead and fan complex, Lanark, Ontario, Canada. *Sediment. Geol.* 72, 285–314.
- Gregoire, L.J., Payne, A.J., Valdes, P.J., 2012. Deglacial rapid sea-level rises caused by ice-sheet saddle collapses. *Nature* 487, 219–222.
- Gregoire, L.J., 2010. Modelling the Northern Hemisphere Climate and Ice Sheets during the Last Deglaciation. (Ph.D. thesis). University of Bristol, UK, Unpublished.
- Greenwood, S.L., Clark, C.D., Hughes, A.L.C., 2007. Formalising an inversion methodology for reconstructing ice-sheet retreat patterns from meltwater channels: applications to the British Ice Sheet. *J. Quat. Sci.* 22, 637–645.
- Hsü, K.J., Kelts, K.R. (Eds.), 1984. *Quaternary Geology of Lake Zürich: An Interdisciplinary Investigation by Deep Lake Drilling*, vol. 13. Contributions to Sedimentology, Stuttgart, 210 pp.
- Hubbard, B., Sharp, M.J., Willis, I.C., Neilsen, M.K., Smart, C.C., 1995. Borehole water-level variations and the structure of the subglacial hydrological system of Haut Glacier d'Arolla, Valais, Switzerland. *J. Glaciol.* 41, 572–583.
- Josephans, H.W., Zevenhuizen, J., 1990. Dynamics of the Laurentide Ice Sheet in Hudson Bay, Canada. *Mar. Geol.* 92, 1–26.
- Joughin, I., Das, S.B., King, M.A., Smith, B.E., Howat, I.A., Moon, T., 2008. Seasonal speedup along the western flank of the Greenland Ice Sheet. *Science* 320, 781–783.
- Kamb, B., 2001. Basal zone of the West Antarctic ice streams and its role in lubrication of their rapid motion. In: Alley, R.B., Bindschadler, R.A. (Eds.), *The West Antarctic Ice Sheet: Behaviour and Environment*. American Geophysical Union, Washington, DC, pp. 157–199. (Antarctic Research Series 77).
- Kleman, J., 1992. The palimpsest glacial landscape in Northwestern Sweden. Late Weichselian Deglaciation landforms and traces of older west-centred ice sheets. *Geogr. Ann., Ser. A: Phys. Geogr.* 74, 305–325.
- Kor, P.S.G., Shaw, J., Sharpe, D.R., 1991. Erosion of bedrock by subglacial meltwater, Georgian Bay, Ontario: a regional view. *Can. J. Earth Sci.* 28, 623–642.
- Kozłowski, A.L., Kehew, A.E., Bird, B.C., 2005. Outburst flood origin of the Central Kalamazoo River Valley, Michigan, USA. *Quat. Sci. Rev.* 24, 2354–2374.
- Lesemann, J.-E., Brennand, T.A., 2009. Regional reconstruction of subglacial hydrology and glaciodynamic behaviour along the southern margin of the Cordilleran Ice Sheet in British Columbia, Canada and northern Washington State, USA. *Quat. Sci. Rev.* 28, 2420–2444.
- Lian, O.B., Hicock, S.R., 2001. Lithostratigraphy and limiting optical ages of the Pleistocene fill in Fraser River valley near Clinton, south-central British Columbia. *Can. J. Earth Sci.* 38, 839–850.
- Lister, G.S., 1984. Deglaciation of the Lake Zürich area: a model based on the sedimentological record. In: Hsü, K.J., Kelts, K.R. (Eds.), *Quaternary Geology of Lake Zürich: An Interdisciplinary Investigation by Deep Lake Drilling*, vol. 13. Contributions to Sedimentology, Stuttgart, 177–186.
- Livingstone, S.J., Clark, C.D., Woodward, J., 2013. Predicting and investigating subglacial lakes and meltwater drainage pathways beneath the Antarctic and Greenland ice sheets. *Cryos. Discuss.* 7, 1177–1213.
- Livingstone, S.J., Clark, C.D., Piotrowski, J.A., Tranter, M., Bentley, M.J., Hodson, A., Swift, D.A., Woodward, J., 2012. Theoretical framework and diagnostic criteria for the identification of palaeo-subglacial lakes. *Quat. Sci. Rev.* 53, 88–110.
- Lopes, C., Mix, A.C., 2009. Pleistocene megafloods in the northeast Pacific. *Geology* 37, 79–82.
- MacAyeal, D.R., 1993. Binge/Purge oscillations of the Laurentide Ice Sheet as a cause of the North Atlantic's Heinrich events. *Paleoceanography* 8, 775–784.
- Marshall, S.J., Clarke, G.K.C., 1999. Modelling North American freshwater runoff through the last glacial cycle. *Quat. Res.* 52, 300–315.
- Margold, M., Jansson, K.N., Kleman, J., Stroeven, A.P., 2011. Glacial meltwater landforms of central British Columbia. *J. Maps* 7, 486–506.
- Margold, M., Jansson, K.N., Kleman, J., Stroeven, A.P., 2013. Lateglacial ice dynamics of the Cordilleran Ice Sheet in northern British Columbia and southern Yukon

- Territory: retreat pattern of the Liard Lobe reconstructed from the glacial landform record. *J. Quat. Res.* 28, 180–188.
- Miyamoto, H., Komatsu, G., Baker, V.R., Dohm, J.M., Ito, K., Tosaka, H., 2007. Cataclysmic flooding: insights from a simple depth-averaged numerical model. *Environ. Modell. Software* 22, 1400–1408.
- Mullins, H.T., Hinchey, E.J., 1989. Erosion and infill of New York Finger Lakes: implications for Laurentide ice sheet deglaciation. *Geology* 17, 622–625.
- Mullins, H.T., Hinchey, E.J., Wellner, R.W., Stephens, D.B., Anderson Jr., W.T., Dwyer, T.R., Hine, A.C., 1996. Seismic stratigraphy of the Finger Lakes: a continental record of Heinrich Event H-1 and Laurentide ice sheet instability. In: Mullins, H. T., Eyles, N. (Eds.), *Subsurface Geological Investigations of New York Finger Lakes: Implications for Late Quaternary Deglaciation and Environmental Change*. Geological Society of America Special Paper, Boulder, Colorado, pp. 311.
- Munro-Stasiuk, M.J., 1999. Evidence for water storage and drainage at the base of the Laurentide ice sheet, south-central Alberta, Canada. *Ann. Glaciol.* 28, 175–180.
- Muller, E.H., Cadwell, D.H., 1986. Surficial geologic map of New York — Finger Lakes sheet: Albany, New York State Museum, Geological Survey Map and Chart Series no. 40, 1 sheet, scale 1:250,000.
- Munro-Stasiuk, M.J., 2003. Subglacial Lake McGregor, south-central Alberta, Canada. *Sediment. Geol.* 160, 325–350.
- Mullins, H.T., Eyles, N., Hinchey, E.J., 1990. Seismic reflection investigation of Kalamalka Lake: a "fjord-lake" on the Interior Plateau of southern British Columbia. *Can. J. Earth Sci.* 27, 1225–1235.
- Pair, D.L., 1997. Thin film, channelized drainage, or sheetfloods beneath a portion of the Laurentide Ice Sheet: an examination of glacial erosion forms, northern New York State, USA. *Sediment. Geol.* 111, 199–215.
- Peltier, W.R., 2004. Global glacial isostasy and the surface of the ice-age Earth: the ICE-5G (VM2) model and GRACE. *Annu. Rev. Earth Planet. Sci.* 32, 111–149.
- Petruccione, J.L., Wellner, R.W., Sheridan, R.E., 1996. Seismic reflection investigations of Montezuma wetlands, central New York State: evolution of a Late Quaternary subglacial channel system. In: Mullins, H.T., Eyles, N. (Eds.), *Subsurface Geological Investigations of New York Finger Lakes: Implications for Late Quaternary Deglaciation and Environmental Change*. Geological Society of America Special Paper, Boulder, Colorado, pp. 311.
- Pugin, A., 1989. Facies model for deglaciation in an overdeepened alpine valley (Bulle area, western Switzerland). *Palaeogeogr. Palaeoclimatol. Palaeoecol.* 70, 235–248.
- Punkari, M., 1997. Glacial and glaciofluvial deposits in the interlobate areas of the Scandinavian Ice Sheet. *Quat. Sci. Rev.* 16, 741–753.
- Prest, V.K., Grant, D.R., Rampton, V.N., 1968. *Glacial Map of Canada*. Geological Survey of Canada Map 1253A.
- Rahmstorf, S., 1995. Bifurcations of the Atlantic thermohaline circulation in response to changes in the hydrological cycle. *Nature* 378, 145–149.
- Ritz, C., Rommelaere, V., Dumas, C., 2001. Modeling the evolution of Antarctic ice sheet over the last 420,000 years: implications for altitude changes in the Vostok region. *J. Geophys. Res.: Atmospheres* 106, 31943–31964.
- Ross, M., Lajeunesse, P., Kosar, K.G.A., 2011. The subglacial record of northern Hudson Bay: insights into the Hudson Bay Ice Stream catchment. *Boreas* 40, 73–91.
- Russell, H.A.J., Arnott, R.W.C., Sharpe, D.R., 2003. Evidence for rapid sedimentation in a tunnel channel, Oakes Ridges Moraine, southern Ontario, Canada. *Sediment. Geol.* 160, 33–55.
- Shaw, J., 1983. Drumlin formation related to inverted melt-water erosional marks. *J. Glaciol.* 29, 461–479.
- Shaw, J., Kvill, D., 1984. A glaciofluvial origin for drumlins of the Livingstone Lake area, northern Saskatchewan. *Can. J. Earth Sci.* 21, 1442–1459.
- Shaw, J., Kvill, D., Rains, B., 1989. Drumlins and catastrophic subglacial floods. *Sediment. Geol.* 62, 177–202.
- Shaw, J., Gilbert, R., 1990. Evidence for large-scale subglacial meltwater flood events in southern Ontario and northern New York State. *Geology* 18, 1169–1172.
- Shaw, J., Munro-Stasiuk, M., Sawyer, B., Beaney, C., Lesemann, J.-E., Musacchio, A., Rains, B., Young, R.R., 1999. The channelized scablands: back to Bretz. *Geology* 27, 605–608.
- Shilts, W.W., Aylsworth, J.M., Kaszycki, C.A., Klassen, R.A., 1987. Canadian shield. In: Graf, W.L. (Ed.), *Geomorphic Systems of North America*, vol. 2. Geological Society of America Bulletin, Centennial Special, vol. 2, pp. 119–161.
- Shreve, R.L., 1972. Movement of water in glaciers. *J. Glaciol.* 11, 205–214.
- Shoemaker, E.M., 1999. Subglacial water-sheet floods, drumlins and ice-sheet lobes. *J. Glaciol.* 45, 201–213.
- Siegert, M.J., Le Brocq, A., Payne, A., 2007. Hydrological connections between Antarctic subglacial lakes and the flow of water beneath the East Antarctic Ice Sheet. In: Hambrey, M.J., Christoffersen, P., Glasser, N.F., Hubbard, B.P. (Eds.), *Glacial Sedimentary Processes and Special Publication*, vol. 39. Oxford, Blackwell Publishing, International Association of Sedimentologists, pp. 3–10.
- Smith, A.M., Murray, T., Nicholls, K.W., Makinson, K., Adalgeirsdóttir, G., Behar, A.E., Vaughan, D.G., 2007. Rapid erosion, drumlin formation, and changing hydrology beneath an Antarctic ice stream. *Geology* 35, 127–130.
- Smith, B.E., Fricker, H.A., Joughin, I.R., Tulaczyk, S., 2009. An inventory of active subglacial lakes in Antarctica detected by ICESat (2003–2008). *J. Glaciol.* 55, 573–595.
- Stearns, L.A., Smith, B.E., Hamilton, G.S., 2008. Increased flow speed on a large East Antarctic outlet glacier caused by subglacial floods. *Nat. Geosci.* 1, 827–831.
- Tarasov, L., Peltier, W.R., 2005. Arctic freshwater forcing of the Younger Dryas cold reversal. *Nature* 435, 662–665.
- Tarasov, L., Dyke, A.S., Neal, R.M., Peltier, W.R., 2012. A data-calibrated distribution of deglacial chronologies for the North American ice complex from glaciological modelling. *Earth Planet. Sci. Lett.* 315–316, 30–40.
- Vanderburgh, S., Roberts, M.C., 1996. Depositional systems and seismic stratigraphy of a Quaternary basin: north Okanagan Valley, British Columbia. *Can. J. Earth Sci.* 33, 917–927.
- Waitt Jr., R.B., 1980. About 40 last-glacial Lake Missoula jökulhlaups through southern Washington. *J. Geol.* 88, 653–679.
- Waitt Jr., R.B., 1984. Periodic jökulhlaups from Pleistocene Glacial-Lake Missoula—new evidence from varved sediment in northern Idaho and Washington. *Quat. Res.* 22, 46–58.
- Walder, J.S., Hallet, B., 1979. Geometry of former subglacial water channels and cavities. *J. Glaciol.* 40, 3–15.
- Walder, J.S., 1982. Stability of sheet flow of water beneath temperate glaciers and implications for glacier surging. *J. Glaciol.* 28, 273–293.
- Winsborrow, C.M., Clark, C.D., Stokes, C.R., 2004. Ice streams of the Laurentide Ice Sheet. *Géogr. Phys. Quat.* 58, 269–280.
- Winsborrow, M.C.M., 2007. *Exploring Controls on the Location of Laurentide Ice Streams* (Unpublished Ph.D. thesis). University of Sheffield, UK, 313 pp.
- Wright Jr., H.E., 1973. Tunnel valleys, glacier surges, and subglacial hydrology of the Superior Lobe, Minnesota. *Geol. Soc. Am. Mem.* 136, 251–276.
- Wright, A.P., Siegert, M.J., Le Brocq, A.M., Gore, D.B., 2008. High sensitivity of subglacial hydrological pathways in Antarctica to small ice-sheet changes. *Geophys. Res. Lett.* 35, L17504.
- Wright, A., Siegert, M.J., 2011. The identification and physiographical setting of Antarctic subglacial lakes: an update based on recent advances. In: Siegert, M.J., Kennicutt, C., Bindschadler, B. (Eds.), *Subglacial Antarctic Aquatic Environments*. AGU Monograph, Washington, DC.